AD-A130 102 NUCLEAR MAGNETIC RESONANCE GYROSCOPE(U) HUGHES RESEARCH 1/1
LABS MALIBU CA D M PEPPER ET AL. APR 83
AFOSR-TR-83-0574 F49620-82-C-0095

UNCLASSIFIED F/G 17/7 NL

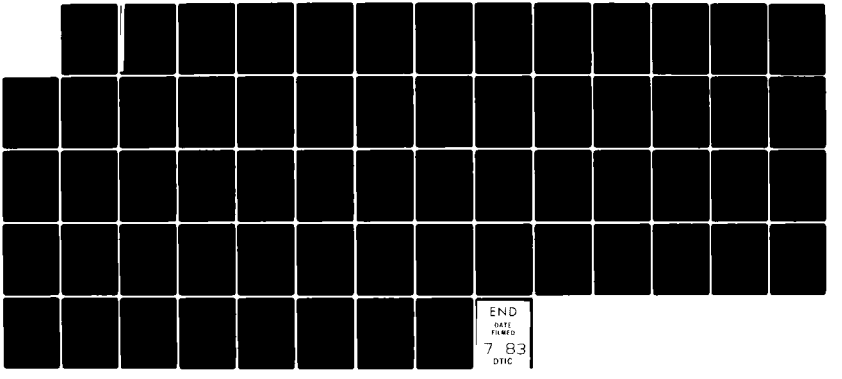

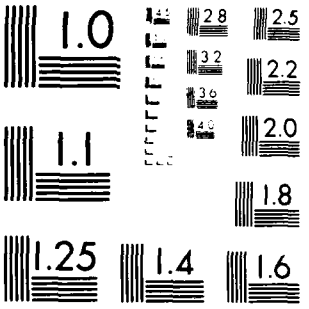

AFOSR-TR- 83-0574

NUCLEAR MAGNETIC RESONANCE GYROSCOPE

D. M. Pepper and H. T. M. Wang

Hughes Research Laboratories
3011 Malibu Canyon Road
Malibu, CA 90265

April 1983

F49620-82-C-0095
Final Technical Report
1 September 1982 through 28 February 1983

Prepared For
AIR FORCE OFFICE OF SCIENTIFIC RESEARCH
Bolling AFB
Washington, DC 20332

UNCLASSIFIED

SECURITY CLASSIFICATION OF THIS PAGE (When Data Entered)

REPORT DOCUMENTATION PAGE	READ INSTRUCTIONS BEFORE COMPLETING FORM
1 REPORT NUMBER: AFOSR-TR- 83-0574	2 GOVT ACCESSION NO. / 3 RECIPIENT'S CATALOG NUMBER
4 TITLE (and Subtitle): NUCLEAR MAGNETIC RESONANCE GYROSCOPE	5 TYPE OF REPORT & PERIOD COVERED: Final Report, 1 Sept. 82 - 28 Feb. 83
	6 PERFORMING ORG. REPORT NUMBER
7 AUTHOR(s): David M. Pepper and Harry T.M. Wang	8 CONTRACT OR GRANT NUMBER(s): F49620-82-C-0095
9 PERFORMING ORGANIZATION NAME AND ADDRESS: Hughes Research Laboratories, 3011 Malibu Canyon Road, Malibu, CA 90265	10 PROGRAM ELEMENT, PROJECT, TASK AREA & WORK UNIT NUMBERS: 61102F 2305/B2
11 CONTROLLING OFFICE NAME AND ADDRESS: Air Force Office of Scientific Research, Bolling AFB, Washington, DC 20332	12 REPORT DATE: April 1983
	13 NUMBER OF PAGES: 64
14 MONITORING AGENCY NAME & ADDRESS (if different from Controlling Office)	15 SECURITY CLASS (of this report): UNCLASSIFIED
	15a DECLASSIFICATION DOWNGRADING SCHEDULE

16 DISTRIBUTION STATEMENT (of this Report)

Approved for public release; distribution unlimited.

17 DISTRIBUTION STATEMENT (of the abstract entered in Block 20, if different from Report)

18 SUPPLEMENTARY NOTES

Research sponsored by the Air Force Office of Scientific Research (AFSC), under contract F49620-82-C-0095. The United States Government is authorized to reproduce and distribute reprints for governmental purposes notwithstanding any copyright notation hereon.

19 KEY WORDS (Continue on reverse side if necessary and identify by block number)

Gyroscope, atomic/nuclear magnetism, magnetic resonance, optical pumping, nuclear polarization, noble gases, collison transfer, isotopes.

20 ABSTRACT (Continue on reverse side if necessary and identify by block number)

A study of the physics of a nuclear magnetic resonance gyroscope is described. Experimental results in nuclear polarization and relaxation in ^{3}He are obtained using an optical pumping apparatus and a high resolution rf spectroscopic technique. Significant polarization in excited state neon was observed via collisional transfer from optically pumped helium in a cell filled with a mixture of helium and neon isotopes. The measured polarization was essentially independent of the isotopic

DD FORM 1 JAN 73 1473 EDITION OF 1 NOV 65 IS OBSOLETE

UNCLASSIFIED

SECURITY CLASSIFICATION OF THIS PAGE (When Data Entered)

composition. Moreover, the polarization of helium in the (He - Ne) binary system was not materially perturbed by the addition of the Ne (for our operating fill pressures). A sensitive rf NMR detection apparatus was fabricated and characterized. The required NMR linewidths of a dual-isotope NMRG sensor necessary to meet the required angular rate sensitivities were estimated. Although we were unable to detect the NMR ground state resonances directly, it is shown theoretically that the required rate sensitivities can be satisfied, given the anticipated output power and observed ground state polarization of helium.

TABLE OF CONTENTS

LIST OF ILLUSTRATIONS

SECTION 1

INTRODUCTION AND SUMMARY

This Final report describes a study on the physics of the nuclear magnetic resonance gyroscope (NMRG) under Contract F49620-82-C-0095, sponsored by AFOSR, during the period 1 September 1982 to 28 February 1983. Technical efforts on this program have further benefited through additional support provided by internal company research funding. This short-term effort constitutes a continuation of a previous AFOSR contract on the same topic (Contract F49620-80-C-0046, covering the period 1 February 1980 to 31 May 1982).

The NMRG is a device that uses magnetic resonance phenomena to measure inertial rotation rates, which can then be integrated to give angular displacement. Nuclear and/or atomic magnetism, which are inherent properties of certain atomic species, are used as the sensing element to replace the rotating mechanical mass or flywheel of the classical gyroscope. The atomic gyro sensor is expected to be compact and reliable, and unlike its mechanical counterpart, there is no bearing to wear out, eliminating periodic recalibration. This reduced maintenance requirement would lead to significant saving in the life cycle cost.

The operation of the NMRG follows from the fact that a magnetic moment precesses about a magnetic field, H_o, in which it is placed. This Larmor precessing frequency, ω_L, is given by

$$\omega_L = \gamma H_o \quad ,$$

where the gyromagnetic ratio, γ, is a characteristic constant of the atomic species. If a system containing the precessing magnetic moment is itself rotating at an angular velocity, ω_r, about the direction of H_o, then observed precession frequency is shifted to

$$\omega = \gamma H_o - \omega_r \quad .$$

Thus, the inertial rotation rate, ω_r, can be inferred from a precise measurement of the Larmor precession frequency of a given magnetic moment in a known magnetic field, H_o. In practice, a magnetic field tends to drift. A closed-loop servo control is required to obtain a certain degree of stability. For this reason, it is necessary to have a second species with a different magnetic moment in the gyro sensor. By observing two magnetic resonances simultaneously in the same magnetic field, the effect of field fluctuations can be eliminated.

Currently, several NMRG designs are under investigation. Each suffers from one or more fundamental problems. These are related to the practice of creating nuclear polarization by optical pumping and observing the nuclear magnetic resonance (NMR) in the same optical pumping cell. Several detrimental effects are incurred by using this approach. First, systematic NMR frequency shifts have been observed. These are caused by real and virtual transitions in the optical pumping cycle or by interatomic collisions (such as spin exchange and metastability exchange collisions[2]) associated with the processes of creating nuclear polarization. Second, such processes also produce line broadening,[1,2] which prevents the full potential of long nuclear relaxation times from being realized. The third problem involves the use of atomic species possessing a nuclear electric quadrupole moment in the presence of alkali or metallic vapors. In one design, nuclear polarization in ground-state noble gas atoms is obtained by collision transfer from optically pumped rubidium vapor, and another employs optically pumped mercury isotopes. In each case, an isotope with a nuclear spin greater than 1/2 (and hence possessing a nuclear electrical quadrupole moment) is used in the dual isotope NMRG sensor. The species possessing a quadrupole moment is sensitive to electric-field-gradient-induced relaxation. In this regard, the condensation of metallic vapors on the walls of the optical pumping cell makes the system non-isotropic. Indeed, orientation-dependent nuclear

relaxation has been observed.[3] This is unsatisfactory for an inertial rotation sensor.

A gyro sensor that uses optically pumped helium isotopes has also been considered. The reference atomic transitions are provided by the ground state NMR in ^{3}He and a Zeeman transition in metastable ^{4}He. Since the metastable lifetime is limited by wall and/or interatomic collisions, the resultant linewidth can be appreciable, thus limiting the ultimate angular rate resolution of the NMRG sensor.

To overcome the problems encountered in current designs, we have conceived a novel NMRG sensor geometry in which optical pumping and NMR observations are conducted in separate but connected regions, as shown schematically in Figure 1. This novel dual-chamber configuration is referred to as the "dumbbell geometry" (in reference to its characteristic shape) and provides separation that will effectively prevent the systematic frequency shift and line-broadening phenomena in the observed NMR transitions. This geometry was first used successfully in a self-sustained oscillating ^{3}He nuclear Zeeman maser,[4] and has since been utilized by other experimenters[5,6] in subsequent ^{3}He polarization studies.

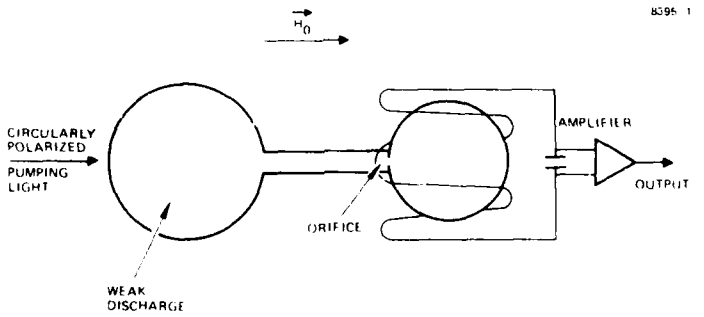

Figure 1. NMR gyro sensor with separated regions for optical pumping and NMR observation.

Using the above geometry, we propose to use two odd-mass-numbered noble gas isotopes as the working materials. Since the ground state of the noble gas atoms possesses a closed electronic shell configuration, their nuclear moments are effectively shielded from external perturbations, resulting in long nuclear relaxation times (and, therefore, narrow NMR linewidths). This fact enables the polarized ground-state atoms to diffuse from the optical pumping region to the NMR observation region of the dumb-bell geometry without appreciable loss of polarization.[4] Furthermore, a system using only noble gas atoms should minimize, if not completely eliminate, the orientation-dependent relaxation phenomenon observed in systems containing a nuclear electric quadrupole moment in the presence of a metallic vapor (as discussed above). Two combinations of noble gas isotopes have been selected for study as possible NMRG sensors.

First, the odd-mass-numbered xenon isotopes, ^{129}Xe and ^{131}Xe, have been selected as the working materials because of the advantage of creating nuclear orientation in both isotopes using a common resonant optical pumping lamp, and becausethe ground-state nuclear relaxation times for these naturally abundant isotopes have been measured to be greater than 20 min.[7]

Second, the dual-isotope combination of ^{3}He and ^{21}Ne has been selected for this study, since ^{3}He, with a ground-state nuclear polarization as high as 40% obtained by optical pumping and a measured nuclear relaxation time of nine days, offers the most desirable attributes for an NMRG sensor. In addition, the low polarizability of neon compared to other heavier noble gases[8] is expected to result in a long nuclear relaxation time. Also, the polarization of ground state ^{21}Ne by optical pumping[9] and of excited states via collisions with optically pumped helium in a ^{4}He-^{20}Ne discharge has been observed.[10] The availability of high isotope enrichment (99.9% + for ^{3}He, and 90% for ^{21}Ne) for these isotopes is an additional advantage. Systems using only noble gases will enable rapid warm-up times for operation of potential tactical NMRG devices.

During the previous program, we designed and successfully constructed an experimental apparatus to study magnetic resonances of optically pumped noble gases using optical detection techniques. Initial efforts were directed to the observation of resonances in helium-3 (^{3}He). Being the least complex noble gas (i.e., a closed s-shell configuration), ^{3}He possesses a nuclear spin (I) of 1/2 and has the smallest polarizability, and hence the longest nuclear polarization relaxation time of the noble gases. Also, ^{3}He can be readily obtained with isotopic enrichments in excess of 99.999%, providing extremely pure samples, essentially free of relaxation-inducing collisions with foreign gases.

After successful system checkout of ^{3}He, efforts were directed to the study of optical pumping of the heavy noble gases, Ne and Xe. Based on the result of this study, we then concentrated our attention on the binary system of ^{3}He and ^{21}Ne.

Highlights of our progress in the previous program include the following:

- Construction of a multinoble gas (^{3} ^{4}He, NAT, ^{21}Ne, NAT, ^{129} ^{131}Xe) gas handling/lamp filling facility.
- Fabrication and successful operation of He, Ne, and Xe pump lamps.
- Fabrication and successful operation of isotopically enriched He, Ne, and Xe single and binary mixture filled absorption cells.
- Fabrication and initial checkout of dual-chamber absorption cells, filled with single and binary mixtures of isotopically enriched noble gases.
- Construction of an experimental apparatus (including magnetic field current source, electronics, pump lamp intensity servo system, optical and rf detection system, and optical components) for studying the various Zeeman resonances.

- Observation of ground state ^3He (as well as metastable and ionic ^3He) Zeeman resonances using two different techniques: (1) changes in ^4He pump light transmission through a ^3He absorption cell; and (2) changes in the optical polarization state of a selected ^3He absorption cell fluorescence line.

- Observation of the "storage" of ground state, polarized ^3He atoms in a dual-chamber absorption cell.

- Observation of an rf "opto-galvanic" signal caused by metastable ^3He absorption of ^4He photons (at 1.08 μm). The phenomenon has implications for source stabilization in systems using laser pumps.

- Development of the concept of monochromatic optical pumping of selected, isolated two-level transitions of metastable, "heavy," odd-mass numbered, noble gases (e.g., ^{21}Ne, ^{129}Xe, ^{131}Xe).

- Observation of $^3P_2$ metastable Zeeman resonances of heavy noble gases ($^{20,21}Ne$, $^{129,131,132}Xe$) using the respective noble gas pump lamps.

- Observation of polarized excited state $^{20,21}Ne$ atoms, by means of collision transfer from optically pumped $^{3,4}He$ in a binary (He-Ne) mixture; the large measured polarization (~1%) is essentially independent of the isotopic composition used.

The latter result is significant in that only a <u>single</u> optical pumping source (He) is required to simultaneously pump <u>two</u> different atomic species (He and Ne). As discussed above, since this combination represents the most desirable pair of atoms for a tactical NMRG, this experimental result represents a promising step toward its realization.

The major thrust of the current program was to construct an apparatus capable of detecting ground-state polarization in single and binary optically pumped noble gas species. This was to be accomplished using direct rf NMR detection techniques.

Furthermore, additional information regarding the polarization transfer scheme in He-Ne mixtures was considered.

Highlights of progress in the current program include:

- Evaluation of the degree of polarization in both He and Ne via optical pumping in binary He-Ne mixtures [at both low (5μm) and high (200 μm) Ne pressures].
- Construction of dual-chamber (^{3}He and He-Ne) absorption cells.
- Observation of the "storage" of polarized ^{3}He atoms in the observation region of dual-chamber absorption cells (consistent with predictions).
- Construction of an rf NMR receiver which is expected to be capable of detecting a ^{3}He polarization of $\sim 10^{-3}$ at a signal-to-noise (S/N) ratio of 2 in a 1 Torr sample.
- Construction of an FET (and also, a reed relay) switching network for use in free-induction decay (FID) studies.

Although we were able to observe the ground-state ($1\,^1S_0$) ^{3}He Zeeman resonance using optical techniques, we were unable to detect this resonance using the direct rf NMR approach. We attribute this to spurious EMI noise sources and, even though we decreased the background noise by more than 30 dB, residual transients produced systematic signals that were on the same order as those expected from the polarized ^{3}He ensemble. However, with improved device performance (further noise reduction, improved field homogeneity, etc.), the detection of rf NMR resonances should be possible.

In the next section, we will describe these accomplishments in greater detail, along with typical results.

SECTION 2

PROGRESS AND EXPERIMENTAL RESULTS

In the first part of this section, we will review the basic physics of the optical pumping process for both ^{3}He and the heavy noble gases. This will be followed by a discussion of optical pumping in binary noble gas mixtures. We will then discuss the experimental apparatus that we have fabricated during this program. Subsequent portions will deal with typical experimental results that we have obtained, and conclude with directions for further experimental efforts.

A. OPTICAL PUMPING OF SINGLE NOBLE GAS SPECIES

In this section we will describe the basic physics that relates to the optical pumping of single, noble gas species.

We limit the discussion here to ^{3}He for several reasons: First, the basic physics of the optical pumping of ^{3}He is well understood. Moreover, the most promising pair of odd-massed isotopes in an NMRG sensor involves the direct optical pumping of ^{3}He. For a more thorough discussion of ^{3}He and the heavy noble gases, the reader is referred to a previous report on NMRG sensors.[1]

The pertinent energy levels for optical pumping of ^{3}He are shown in Figure 2. A schematic of the basic optical pumping apparatus is shown in Figure 3. Metastable 2^3S_1 atoms are created by a weak discharge in a sample of ^{3}He at a pressure of about 1 Torr. The sample thus contains a mixture of ground state and metastable atoms, as well as other discharge products. Typically, the ratio of ground-to-metastable state atom density is approximately 10^6:1. Circularly polarized light at 1.08 μm from a ^{4}He lamp incident collinearly with an externally applied magnetic field will selectively excite the $2^3S_1 \rightarrow 2^3P_0$ transition according to the selection rule, $\Delta m = +1$ (or -1, depending on the sense of polarization). A ^{4}He lamp is chosen for its favorable

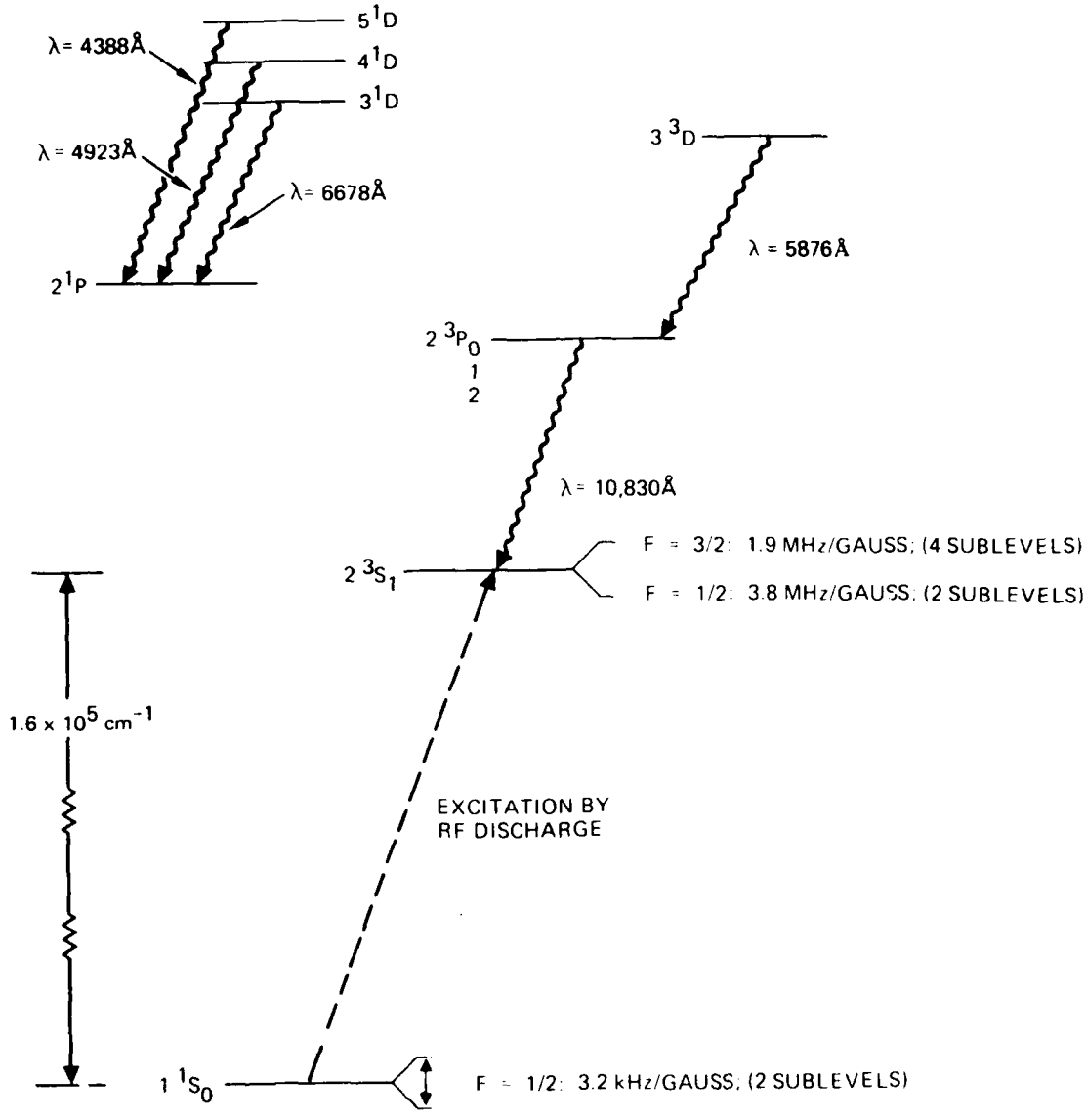

Figure 2. Energy level diagram pertinent to the optical pumping of ^3He. Also shown are the magnetic-field dependence of relevant hyperfine sublevels.

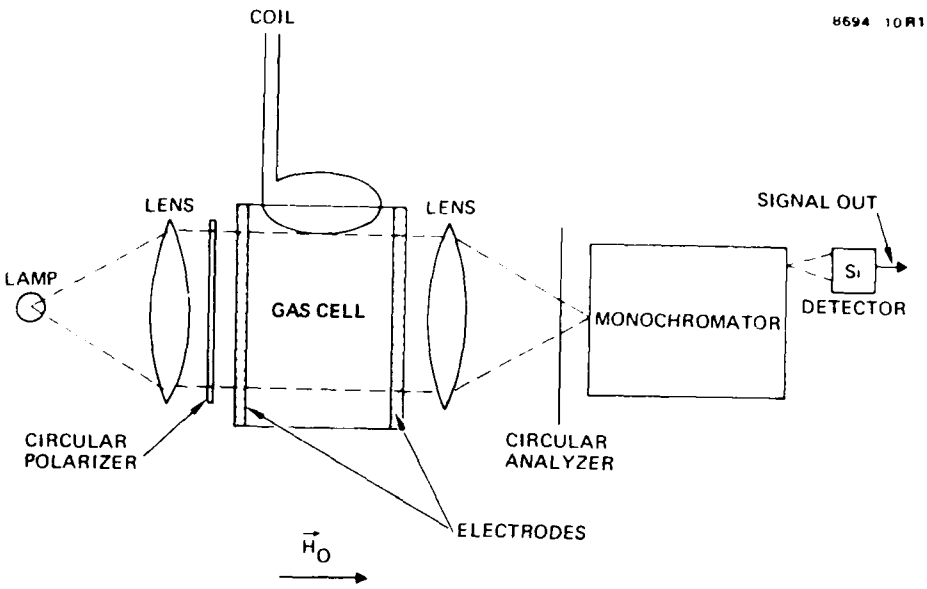

Figure 3. Schematic of an optical pumping apparatus.

isotope shift.[1] Thus, the optically pumped ^{3}He metastables will become polarized (i.e., a population difference of Zeeman sublevels far in excess of the Boltzmann distribution will result). Metastables in a collison with a neutral atom have a large cross section[12] (~7 x 10^{-16} cm^2) for exchange of metastability. Since angular momentum is conserved in such collisions, the metastable polarization is efficiently transferred to the ^{3}He ground state ($1\,^1S_O$) nuclear orientation. The tight coupling between the directly pumped metastables and the ground state through metastability exchange results in a large ground-state nuclear polarization. Moreover, as a result of the closed s-shell electronic configuration, the nuclear moment is well shielded from external perturbations. Hence, extremely long nuclear relaxation times can be realized under proper conditions, such as isolating the optical pumping and the NMR observation regions (using the dumbbell geometry).

The tight coupling between the ground-state nuclear orientation and the metastable polarization enables the ground-state NMR to be conveniently detected by monitoring the changes in transmitted pump light intensity as a test signal is coupled to the absorption cell at the Larmor precession frequency. Alternately, the signal-to-noise (S/N) ratio can be improved by monitoring the optical polarization asymmetry of certain excited-state transitions. Since only a specific wavelength is of interest, a narrow bandpass interference filter can be used to suppress the background level. The physical mechanism responsible for this detection scheme is that the ground-state nuclear orientation, which serves as a reservoir of angular momentum, is coupled to the excited states by atomic collision processes. The polarization of the excited state fluorescence can be measured with high sensitivity by a circular polarization analyzer consisting of a rotating quarter-waveplate (which can be realized either mechanically or electro-optically), followed by a linear polarizer and an optical detector (e.g., a photo-multiplier). Examples of excited state transitions in helium that can be conveniently used to monitor ground-state nuclear orientation are the ($2^1P \rightarrow 3^1D$) and ($2^3P \rightarrow 3^3D$) transitions at 6,678 Å and 5,876 Å, respectively (see Figure 2). Our apparatus was constructed to monitor the former fluorescence line. Our successful results will be discussed in Section 2.E.

The use of optical detection techniques to monitor Zeeman resonances in the noble gases require the sample to be driven by a (weak) discharge. This is due to the fact that the optical detection schemes discussed above involve probing a metastable level or monitoring excited-state fluorescence. The presence of discharge products (ions, electrons, etc.), coupled with the finite lifetime of the metastable levels, reduces the polarization lifetime, and hence, increases the linewidth of the

observed resonances. This detection technique would therefore limit the performance of an NMRG sensor.

These limitations can be circumvented by utilizing the proposed dual-chamber geometry. In this case, the observation region contains only ground-state atoms (both polarized and unpolarized atoms). Hence, being free of discharge-induced relaxation processes, the resultant polarization lifetimes can be very long, resulting in improved device performance.

For the dumbbell geometry, separating the optical pumping and the NMR observation regions requires that an rf method similar to conventional NMR techniques be used. In this case, the NMR can be detected through changes in the reactance of an rf resonance circuit coupled to the oriented spin when the nuclear Zeeman transition is stimulated.

The basic components of this scheme are shown in Figure 1. A carefully wound coil which surrounds the observation region of the dumbbell assembly is arranged in conjunction with a capacitor capacitor to form a tuned circuit. The Q of this tuned circuit can be made in the range of 200-300 for the resonant frequencies chosen for our study (~3 kHz to 40 kHz); this range was dictated by the available magnetic field apparatus.

The LC circuit is followed by a narrow bandpass, high input impedence amplifier. A switching network allows a stimulating pulse to be coupled into the coil, which coherently prepares the atoms to radiate.

When stimulated, the polarized atomic ensemble coherently radiates at the Larmor frequency, coupling energy into the LC network. The atomic ensemble can be viewed as an array of current loops (i.e., oscillating, magnetic moments) that induces an EMF, $\mathcal{E}$, in the LC network. This induced signal can be shown[13] to be

$$\mathcal{E} = N_r A_r \omega \mu_o M \cos(\gamma B_o t) \quad ,$$

where

$$M = N \langle \mu_z \rangle \quad .$$

Here, N_r and A_r is the number of turns and area of the receiver coil, respectively; M is the magnetization, N is the number density of polarized atoms, B_o is the applied static magnetic field and γ is the gyromagnetic ratio. $\langle \mu_z \rangle$ is the expectation value of the z-component of the magnetic moment of the atomic species.

Using the above relationship, we anticipate an induced EMF on the order of $\sim 10^{-5}$ V for our experimental parameters. This value is consistent with that estimated using a photon energy conservation calculation where

$$P \cong \frac{Nh\gamma B_o}{t} \quad .$$

Here, P is the power radiated by an atomic ensemble composed of N polarized atoms, radiating at frequency γB_o over a time interval, t. Assuming a radiative lifetime of 1 second, a geometrical filling factor of 1% and a 50-Ω impedence, leads to a level of $\sim 10^{-5}$ V, in agreement with the above calculation.

The estimated lifetime of 1 second gives rise to very narrow resonance linewidths, resulting in a large atomic line Q, Q_a, of $\sim 10^4$ (at a resonance frequency of 10 kHz). This enables one to realize NMRG rotational rate sensitivities consistent with system requirements. We note that this large value of Q_a is well within the electronic Q of the detection apparatus (coil Q ~200; filter Q ~100).

The radiative lifetime of the polarized ensemble can, however, be made to be much greater than 1 second. The lifetime is ultimately limited by geometrical factors (e.g., the atomic storage time of the dual-chamber absorption cell observation region) and magnetic field relaxation effects (e.g., spatial and temporal field inhomogenities). Thus, even greater rotational rate sensitivities can, in principle, be realized.

In conclusion, we note that such narrow linewidths cannot be realized in an apparatus where the optical pumping and resonance observation simultaneously takes place in the same volume. Hence, one can appreciate the increased device performance afforded by using a geometry with an observation region that is free from discharge-induced relaxation processes. Again, this geometry necessitates rf (as opposed to optical) detection techniques.

B. OPTICAL PUMPING OF BINARY NOBLE GAS MIXTURES

We previously selected a mixture of (^{129}Xe, ^{131}Xe) isotopes as working materials for a dual-isotope NMRG sensor. The selection was based on the expectation that ground-state nuclear polarization can be created in both isotopes using a common resonant pumping source. This would lead to a compact device, which is desirable in real applications. On the other hand, the relatively large depolarization cross section for metastable xenon,[14]

$$\sigma(Xe^m - Xe) = 190 \times 10^{-16}\ cm^2 \quad ,$$

compares rather unfavorably with that for metastable neon in a cell using helium as a buffer gas:[10]

$$\sigma(Ne^m - Ne) = 16.6 \times 10^{-16}\ cm^2$$
$$\sigma(Ne^m - He) = 0.43 \times 10^{-16}\ cm^2 \quad .$$

The smaller neon metastable depolarization cross section is caused by the smaller polarizability of neon compared to the heavier noble gases.[8] Moreover, the best isotopic enrichment for the odd-mass-numbered xenon isotopes is only about 60%, while ^{21}Ne is available with a purity of 90%.

The potential for a larger ground-state nuclear orientation and a smaller resonance linewidth for ^{21}Ne compared to the xenon isotopes makes it worthwhile to consider its feasibility for NMRG applications. Specifically, the combination of ^{3}He and ^{21}Ne, for reasons stated earlier, form a favorable pair of working atomic species. At first, one may conclude that because of the different transitions necessary to simultaneously optically pump both species (1.08 μm and 6,402 Å for ^{3}He and ^{21}Ne, respectively), two pump lamps are required. A schematic of such a scheme is shown in Figure 4. The linear three-sphere geometry retains the concept of separated regions of optical pumping (for each isotope) and NMR observation. The added components may constitute disadvantages (e.g., size, weight, energy requirements, and cost) for NMRG applications.

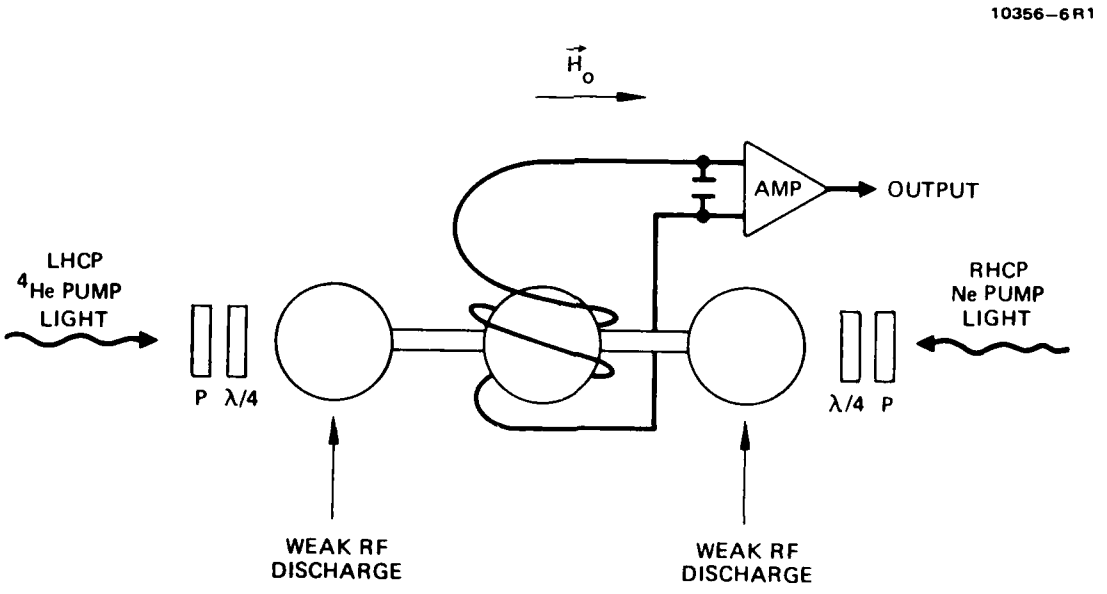

Figure 4. Linear, three-sphere, dual-isotope NMR gyro sensor using separate regions for optical pumping of each isotope and NMR observation.

A possible solution to these disadvantages in the He-Ne system can be realized upon examination of the energy dynamics in He-Ne collisions. The existence of near-resonant energy levels between metastable helium and excited-state neon atoms, as shown in Figure 5, coupled with the operation mechanisms of the He-Ne laser, provides a possible scheme for collison transfer. The polarization of excited levels of neon by collisions with optically pumped helium in an absorption cell has been observed (using a mixture of naturally abundant He and Ne), and in addition, it was shown that the polarization is retained in lower lying neon levels by cascaded radiative transitions.[10] Since the experiment used optical detection techniques involving fluorescence from excited states of neon, the polarization of the $3s^3P_{2\ 0}$ metastable states was not measured. Moreover, because of the large percentage of even isotopes in naturally abundant He and Ne, no ground-state polarization was expected.

In Section E.2, we will describe successful experimental results where significant excited state polarization in both ^{3}He and ^{21}Ne was observed using a single pump lamp (1.08 μm from ^{4}He). The polarization in ^{21}Ne was a factor of five greater than that obtained using direct optical pumping techniques (i.e., 6,402 Å from a Ne pump lamp). In addition, the degree of polarization, within experimental error, was the same in neon, regardless of the isotopic composition of the $^{3\ 4}$He-$^{20\ 21}$Ne mixtures. The excellent S/N ratio observed in excited-state ^{21}Ne resonances leads us to expect that significant metastable ^{21}Ne polarization is present. Hence, one anticipates that significant ^{21}Ne ground-state nuclear orientation can be obtained through metastability exchange collisions. Furthermore, polarization of ground-state ^{3}He was also maintained in the He-Ne mixture, even in the presence of the neon species. In fact, for the partial pressures used, the ^{3}He polarization was measured (within our experimental error) to be the same value using cells with and without neon present. This approach could result in a compact,

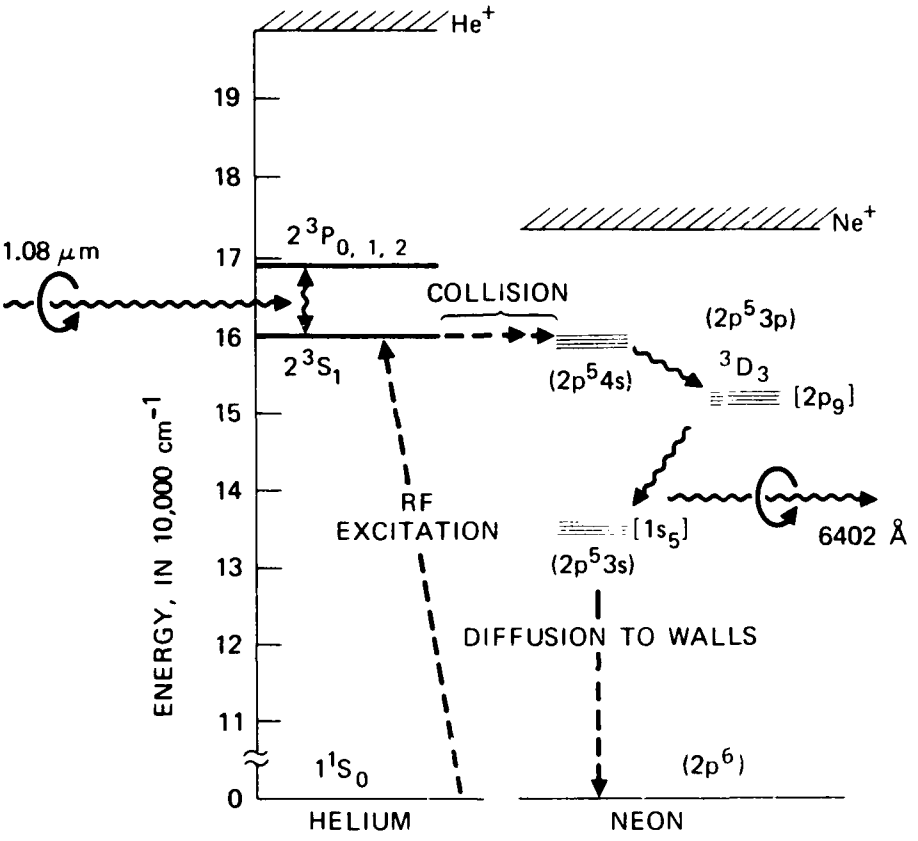

Figure 5. Relevant energy levels in a He-Ne system.

high performance, dual-isotope, all-noble-gas NMRG sensor (using only a single ^{4}He pump lamp), since the desirable features of ^{3}He for NMRG applications are well established.

C. GYRO PERFORMANCE ESTIMATION

The ultimate performance of the dual isotope NMRG sensor depends critically on an ability to measure precisely the NMR frequencies of the two nuclear isotope species and to perform the

required arithmetical operations in order to extract the rotational rate. For the present calculations, we assume the following:

- An angular rate sensitivity of 1°/hr, or $\delta f \cong 0.8 \times 10^{-6}$ Hz;
- an operating dc magnetic field of 1 gauss;
- dual isotopes of ^{3}He and ^{21}Ne in the NMRG sensor;
- polarized atomic storage time of ~30 seconds.

In a dual isotope NMRG sensor using a single, dual-chamber absorption cell, the rotation rate, ω_r, is given by

$$\omega_r = \frac{\gamma_2\omega_1 - \gamma_1\omega_2}{\gamma_1 - \gamma_2} \quad , \tag{1}$$

where γ_i and ω_i are the gyromagnetic ratio and measured resonance frequency of the i^{th} atomic species, respectively. The required precision of the physical constants and the measured resonance frequencies can be estimated as follows. The required mean square fractional rotational rate is given by

$$\left(\delta\omega_r\right)^2 = \sum_i \left(\frac{\partial\omega_r}{\partial x_i}\right)^2 (\delta x_i)^2 \quad , \tag{2}$$

where $x_i = \gamma_1, \gamma_2, \omega_1, \omega_2$.

In the dual isotope NMRG sensor under consideration, ^{3}He and ^{21}Ne are species 1 and 2, respectively. Hence, $\gamma_1 \cong 2\pi \times 3.2 \times 10^3$ rad/gauss and $\gamma_2 \cong 2\pi \times 3 \times 10^2$ rad/gauss. γ_1 and γ_2 are constants for the isotopic species and are known to high precision.

Now, taking the partial derivitives, and requiring that $\delta\omega_r \leq 2\pi \times 0.8 \times 10^{-6}$ Hz, the required fractional frequency precision is

$$\left(\frac{\delta f}{f}\right)_{1,2} \simeq 2.57 \times 10^{-9} \quad . \tag{3}$$

In deriving Equation (3), we have assumed that $\delta\gamma_1 \simeq 5.17 \times 10^{-5}$ and $\delta\gamma_2 \simeq 4.85 \times 10^{-5}$. Recall that the fractional frequency requirements are necessary to realize a NMRG sensor angular rate sensitivity of 1°/hr. We next calculate the value that can be expected, based on anticipated experimental conditions and constraints.

The fractional resonance frequency uncertainty, $\langle \Delta f/f \rangle$, can be related to the atomic resonance quality factor, Q_a, by the equation

$$\left\langle \frac{\Delta f}{f} \right\rangle \simeq \frac{1}{Q_a} \sqrt{\frac{kT}{2P\tau}} \quad , \tag{4}$$

where kT is the thermal energy, τ is the integration time (or the reciprical of the detector bandwidth, $\Delta\nu$), and P is the power radiated by the polarized atoms. This power is given by

$$P \sim \frac{\Gamma}{2} Nphf \quad , \tag{5}$$

where Γ, N, ρ, and f are the relaxation rate of the polarized ensemble, number of atoms, fractional polarization, and resonance frequency, respectively. Assuming 1 Torr of ^{3}He in a volume of 10 cm^3 and a polarization of 10% yields a radiated power, P, $\simeq 10^{-15}$ W.

If we assume a storage time of t_g = 30 seconds, the atomic linewidth is given by $\Delta f_a = 1/(\pi t_g) \sim 10^{-2}$ Hz. Hence, the Q of the atomic system, Q_a, is

$$Q_a = \frac{f}{\Delta f_a} \approx 3.2 \times 10^5 \quad .$$

Using these values of P and Q_a in Equation (4), and assuming a receiver bandwidth of 1 Hz, results in a mean value of the fractional linewidth to be

$$\langle \frac{\Delta f}{f} \rangle \sim 2.3 \times 10^{-9} \quad , \qquad (6)$$

which is on the same order as the required value of $(\delta f/f)_{1,2}$ above. For ^{3}He, this is a conservative estimate in that the ^{3}He storage times approaching 9 days have been measured by other workers.[1] For the heavy noble gas isotope component of the dual isotope NMRG sensor, the technical problem of obtaining a higher nuclear polarization than what has been demonstrated has to be overcome to achieve the desired frequency measurement precision. Nevertheless, we feel that a ^{3}He-^{21}Ne dual isotope NMRG sensor capable of satisfying the assumed angular rate sensitivity is achievable.

D. EXPERIMENTAL APPARATUS AND MEASUREMENT TECHNIQUES

In this section we will describe the optical pumping apparatus we have fabricated, and discuss the observation techniques that were employed. We will concentrate primarily on the rf NMR receiver electronics system. The other major components (e.g., pump lamps, absorption cells, magnetic field apparatus, and optical detection elements) were described in detail in the previous NMRG final report.[11]

1. Experimental Apparatus

As mentioned earlier, the requirement for narrow linewidths of the Zeeman resonances (using our geometry) necessitates a direct rf NMR detection approach. The basic apparatus is sketched in Figure 6 and consists of a receiver coil tank circuit, filters, narrowband amplifier stages, stimulating networks, and an optional phase-shifting network (with associated feedback) for Q-enhanced oscillation studies. (The latter two items will be addressed in the next subsection.) The receiver coil consists of 200 to 1000 turns of #32/40 Litz wire wound in a grounded, center-tapped configuration. The capacitor used to complete the LC network is placed across the outer halves of the coil, which is connected to a high input impedence, low noise, state-of-the-art FET-driven differential amplifier. This configuration enables one to realize extremely high common mode rejection (by virtue of the split coil/differential amplifier network), in conjunction with obtaining high sensitivity ($\sim 10^{-16}$W at a S/N ratio of 2) and selectivity (coil Q ~ 250). The receiver was designed to detect a ^{3}He polarization as low as 10^{-3} at a S/N ratio of 2 at a helium pressure of 1 Torr. A switching network and a shielded low pass filter are situated prior to the differential amplifier input. The switching network is used to inject single or multiple stimulating pulses across the receiver coil for transient polarization measurements (see next section). The low-pass filter is used to prevent RFI (from both the pump lamp and absorption cell rf drivers), as well as other EMI sources and transients from systematically affecting the receiver electronics.

Following the differential amplifier is a series of low-noise, narrowband amplifiers. The Q of this amplifier network was chosen to be ~100 to avoid systematically effecting the receiver coil selectivity, while being high enough to suppress background noise.

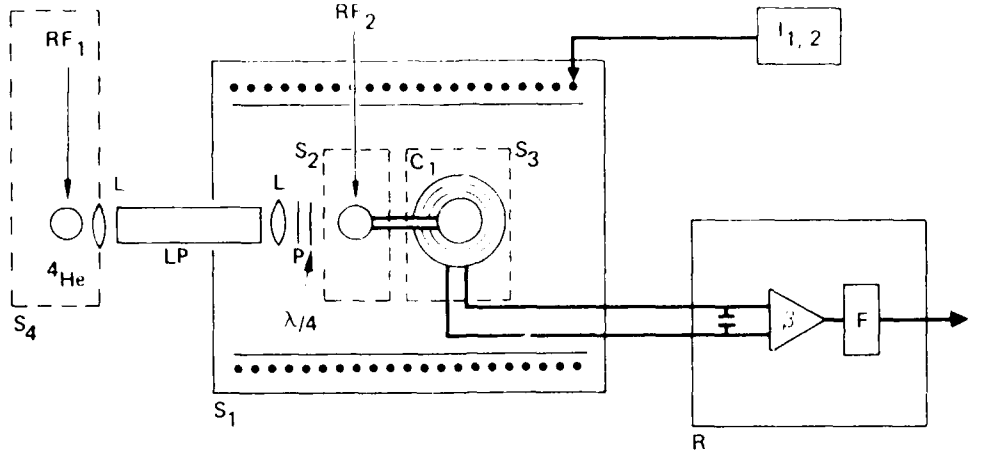

KEY:

RF_1	"STRONG" PUMP LAMP RF DRIVE
RF_2	"WEAK" ABSORPTION CELL RF DRIVE
LP	QUARTZ LIGHT PIPE
L	LENS
P	POLARIZER (AT $\lambda = 1.08\,\mu m$)
$\lambda/4$	QUARTER-WAVE PLATE (AT $\lambda = 1.08\,\mu m$)
S_1	PERMALLOY MAGNETIC SHIELD (3 CONCENTRIC CYLINDERS W/END CAPS)
$S_{2,3}$	COPPER SHIELD (~ 8 mm THICK)
S_4	PUMP LAMP SHIELD
R	NMR RECEIVER
$I_{1,2}$	SOLENOID PRECISION CURRENT SOURCES (MAIN AND SECOND ORDER CORRECTION COILS)
C_1	RECEIVER COIL (Q ~ 250)
F	NARROW BANDPASS FILTER (Q ~ 100)
β	LOW-NOISE AMPLIFIER

Figure 6. Experimental geometry used for rf NMR detection.

The input networks of the various receiver amplifier stages were gated by FET switches, as controlled by the switching network. This enabled the receiver to be isolated from the LC network during the stimulating mode. Finally, care was taken to provide time delays so that the various amplifier stages would be "enabled" in a sequence to minimize FET-induced current transients in the receiver.

The presence of the above rf sources (for the pump lamp and absorption cells), coupled with local line transients, presents an appreciable set of noise sources. This can affect not only the control electronics (e.g., solenoid current supplies, and various servo systems), it can also systematically stimulate the NMR receiver coil and associated rf detection electronics.

To minimize the various noise sources, several techniques were used for both the pump lamp and absorption cell rf drivers. First, the rf apparatus for the pump lamp was housed in a grounded aluminum shield. Then feed-through EMI filters were used to isolate the rf equipment power supply lines from the other laboratory apparatus. An impedance matching network and tuned circuit were used to inductively couple the rf output to the pump lamp. A similar approach was used in conjunction with the absorption cell rf driver. The discharge region of the absorption cell was housed in an 8-mm-thick copper shield (along with a tuned circuit to minimize reflected rf). The walls of the shield were chosen to be several skin depths in thickness at the Larmor frequencies of interest (~3 kHz to ~40 kHz). In addition, for experiments involving the dual-chamber absorption cells, a dual-chamber copper shield was employed to separately shield both the discharge region of the cell and the NMR observation region.

2. Measurement Techniques

There were two optical techniques (in addition to the direct rf NMR approach) that we used to detect the polarization state of

the atoms and the various magnetic resonances. The first technique involves monitoring changes in the transmission of the 1.08 μm pump light through the absorption cell as a result of the application of time-varying fields at the Larmor frequencies. The second approach involves observing corresponding changes in the optical polarization state of an isolated absorption cell fluorescence line and is referred to as the optical polarization asymmetry (OPA) technique. Both of these optical techniques are discussed in detail in the previous NMRG report.[11] The optical detection schemes were used primarily for system and cell checkout purposes.

In addition to the above optical detection schemes, we employed direct rf NMR techniques to search for the various Zeeman resonances. In all cases the dual-chamber absorption cells were employed. The NMR detection technique was used under continuous optical pumping conditions (i.e., both the pump lamp and absorption cell discharges were driven while the observation region was probed), as well as a "quiescent mode" (whereby either or both of the rf sources were turned off after the atoms were optically pumped). The latter case was attempted in order to minimize RFI sources from interferring with the measurements.

Although there are a variety of coherent stimulation techniques available,[12] we employed the free-induction decay scheme to search for the polarized species. In this case, a single (or a series of) rf burst(s) at the Larmor frequency is applied across the receiver coil. The duration of the pulse is chosen to be much less than the anticipated dephasing time (~1 sec) of the polarized atomic ensemble. The amplitude of the rf burst is chosen to give rise to a $\pi/2$ pulse. This choice of time and amplitude places the polarized species in a radiating state, resulting in the so-called free-induction decay (FID) of the magnetic moments. The switching network and associated timing sequence used in our studies is shown in Figures 7 and 8. The basic approach is to isolate (and ground) the various receiver

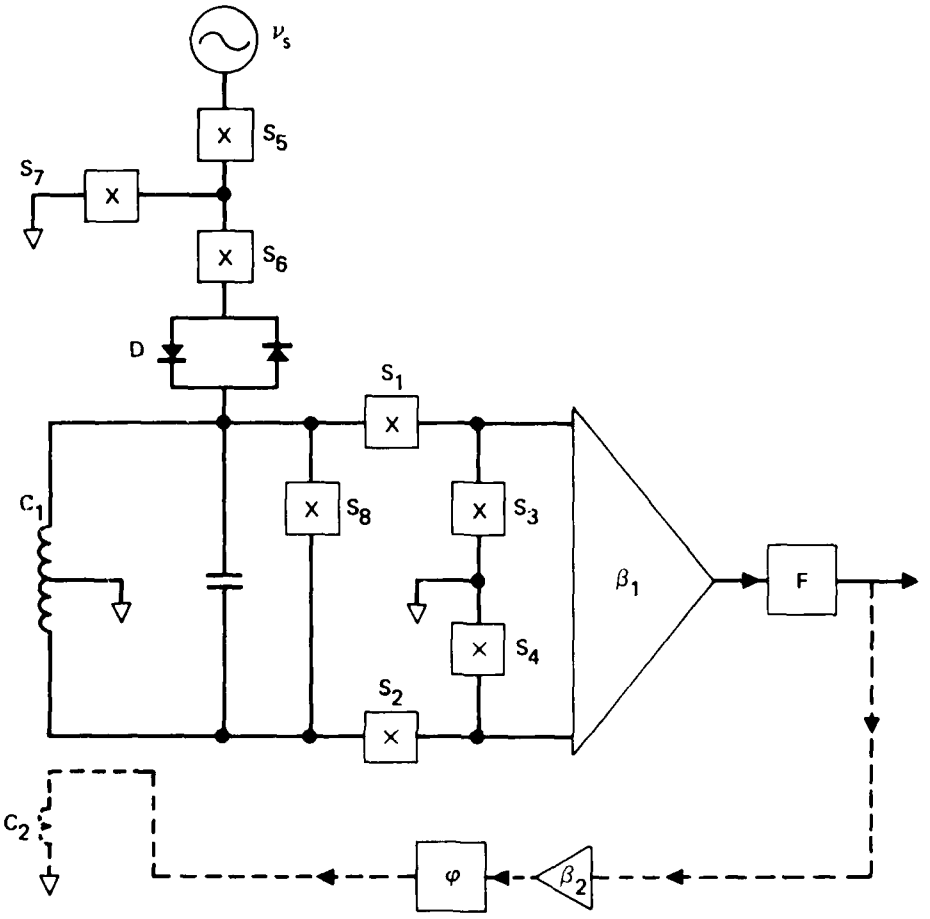

KEY:
- C_1: RECEIVER COIL (Q ~ 250)
- C_2: FEED-BACK COIL (FOR Q-ENHANCED MODE)
- S_i: FET SWITCHES (OR REED RELAYS)
- β_i: LOW-NOISE AMPLIFIERS
- F: NARROW BANDPASS FILTER (Q ~ 100)
- φ: PHASE SHIFTER (ADJUSTABLE)
- ν_s: STIMULATING FREQUENCY OSCILLATOR
- D: BACK-TO-BACK DIODES (FOR ISOLATION)

Figure 7. Block diagram of the NMR receiver, resonant circuitry and switching network.

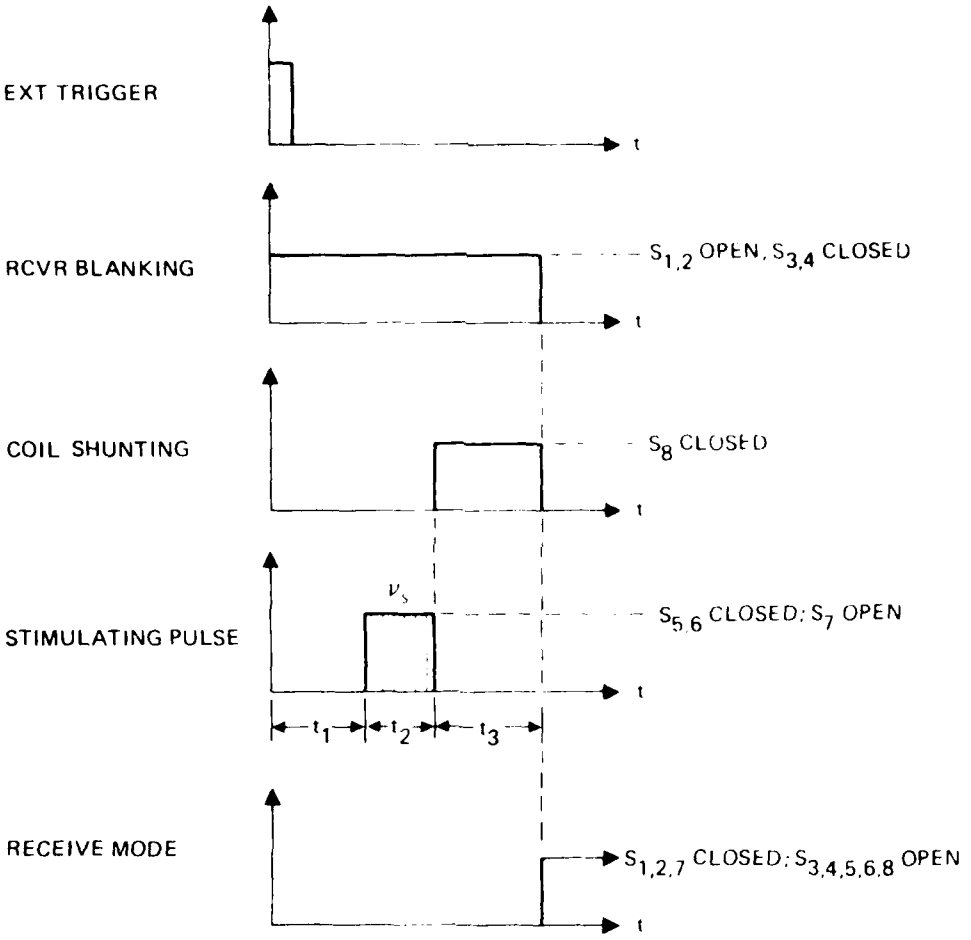

Figure 8. Pulse timing sequence for free induction decay studies.

stages during the stimulation mode. During this time, the output from a frequency synthesizer is gated on and placed across the receiver coil. After application of the stimulation pulse, the receiver coil is shunted; this action temporarily decreases the Q of the coil, thereby damping out any residual ringing of the tank circuit. This is followed by a short blanking period, after which the amplifier stages are enabled, and the LC circuit is switched into the pre-amp input terminals. During this program, both reed relays and the FET switches were used in the switching network. It was noted that the FET switches induced a slight amount of ringing in the system and reduced the Q of the system by approximately 20% (apparently due to capacitive effects).

As presentated in Figures 7 and 8, a typical pulse timing sequence occurs as follows: During the blanking period, the receiver input is protected by opening switches $S_{1,2}$ and closing $S_{3,4}$. During the application of the stimulating pulse, S_5 and S_6 closed and S_7 is opened. The various time periods ($t_{1,2,3}$), as well as the stimulating pulse frequency, ν_S, and amplitude are all adjustable. The receiver Q is spoiled by closing S_8 after the stimulating pulse in order to minimize coil ringing. The back-to-back diodes are used to further isolate the receiver tank circuit from the stimulating pulse apparatus. The NMR receiver was also designed to be capable of operating in a Q-enhanced oscillation mode. In this case, the receiver was operated in a continuous manner, with its output phase shifted, amplified, and coupled back into the receiver coil (using severa turns of Litz wire wound around the receiver coil form). The system was checked out (without the atomic medium) by observing that the receiver output would break into a stable oscillation mode upon proper adjustment of the phase shifter and feedback amplifier gain. During operation, the gain of the feedback amplifier would be adjusted to be marginally below the oscillation threshold, with the additional gain to be provided by

the inverted nuclear moments. Since we were unable to detect the FID signal, this Q-enhanced mode was not employed.

E. EXPERIMENTAL MEASUREMENTS AND RESULTS

In this section, we will discuss the experimental results obtained during this program. As a means of illustration of the experimental techniques discussed above, we will discuss key results obtained during the previous NMRG program with respect to the optical pumping of ^{3}He and the optical pumping of binary mixtures of He and Ne. The section will conclude with a discussion on the attempts to observe polarization in ground state ^{3}He using direct rf NMR techniques.

1. Optical Pumping of Helium

Using ^{3}He as the optically pumped species, we have observed metastable absorption of 1.08 μm pump light from a ^{4}He lamp, leading to significant metastable and ground-state polarization (~9.5%). Both of the optical detection techniques described above were successfully utilized, with the OPA approach permitting us to observe Zeeman resonances in the ionic ground state of ^{3}He, as well as evidence of the "storage" of ground-state polarized ^{3}He atoms in the observation region of a dual-chamber absorption cell.

These techniques were extremely useful in that they verified the existence of polarized ^{3}He atoms. Hence, not only did this serve as a check of our experimental apparatus (i.e., solenoid, pump lamp, absorption cell discharge conditions, detection electronics), it also functioned as a checkout of our absorption cell purity and filling procedure. Thus, prior to searching for for the direct rf NMR signals, each dual-chamber absorption cell was tested by observing and measuring the ground (and metastable) state polarization optically. Moreover, the OPA technique enabled us to establish that polarized ground state atoms were indeed stored in the observation region of the dual-chamber

absorption cells — a necessary condition for the detection of polarization in the observation region using direct rf NMR techniques.

As an example of the pump light transmission technique, we show in Figure 9 the results of a measurement made on an absorption cell containing 900 μm of ^{3}He. In this case, a pump lamp containing ~2 Torr of ^{4}He was used to optically pump the 2^3S_1 state of ^{3}He, as described earlier. The resultant polarization was measured to be ~9.5%. For this run, the resonances were observed by synchronously detecting changes in the transmission of pump light through the absorption cell as an applied magnetic field is slowly scanned. This was done in the presence of two fixed test oscillator frequencies coupled to the absorption cells through a pair of (Larmor) rf coils. The first coil was driven at ~5.7 kHz for the ground-state NMR.* In addition, a second coil, driven at 12.28 MHz, was placed around the absorption cell to couple to several other ^{3}He resonances: the two ^{3}He 2^3S_1 metastable Zeeman resonances at 1.9 MHz/G and at 3.8 MHz/G (corresponding to the F = 3/2 and F = 1/2 sublevels, respectively); and the $1^2S_{1/2}$ resonance of the ground ionic state of ^{3}He ($^3He^+$) at 1.4 MHz/G. For this run, the magnetic field was scanned from ~1 to 10 G at a rate of ~1 G/min. The lock-in integration time was 4 sec. To calibrate the magnetic field, the ground-state neutral ^{3}He Larmor resonance coil was driven by a square wave. The presence of the resultant odd harmonics made coupling to the 1^1S_0 nuclear resonance possible as the magnetic field (H) was swept through its range (i.e., at H_0, $3H_0$, $5H_0$, etc.). In addition to these signals (corresponding to the ground-state resonance), both of the 2^3S_1 resonances are seen. The increased width of the latter resonances is due to the smaller metastable helium (^{3}He*)

---

*The Larmor coil frequencies were chosen so that the various resonances could be observed over our magnetic field sweep range.

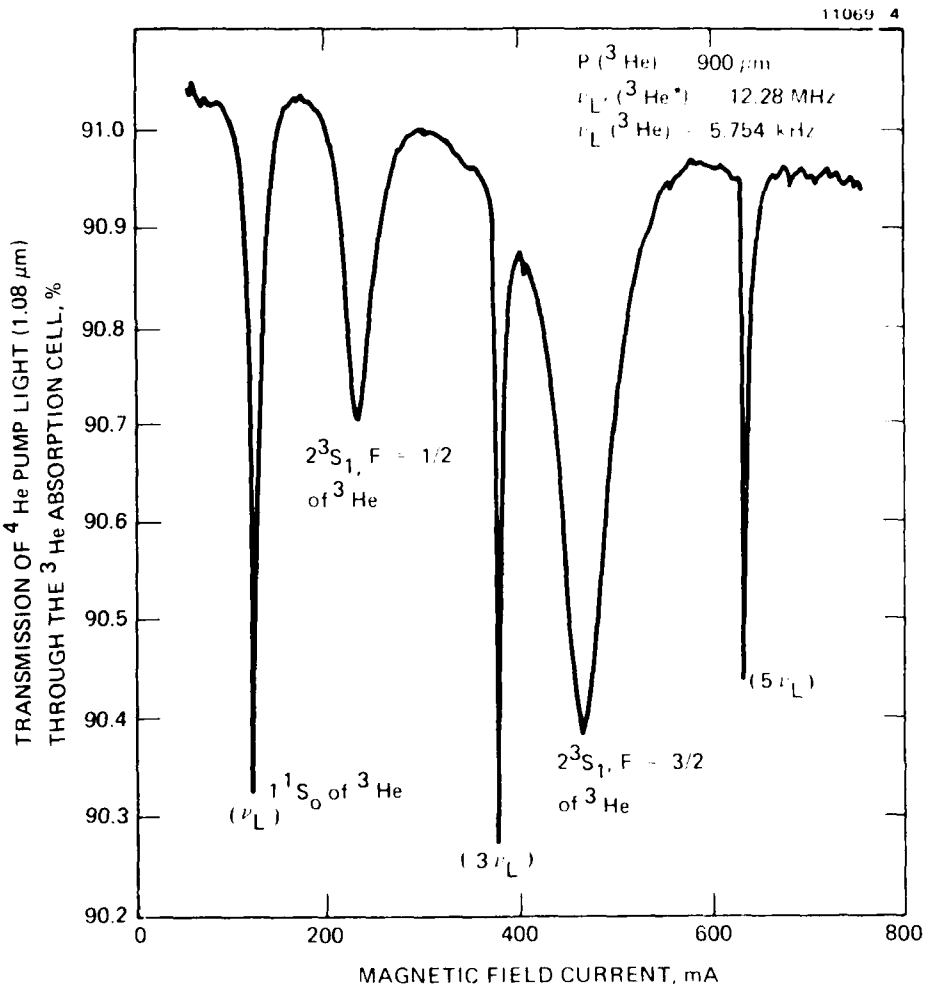

Figure 9. Observation of ^{3}He (ground state and metastable) resonances by scanning the applied magnetic field and monitoring the pump light transmission.

lifetime, which is dominated by metastabililty exchange collisions. The widths of the resonances cannot be precisely determined from these data. For such a determination, it is necessary to take into account the magnetic field scan rate and the detection system integration time.

The use of the optical polarization asymmetry (OPA) technique for the detection of magnetic resonance is important in that it can yield a higher S/N ratio. Here, changes in the circular polarization state of an isolated absorption cell fluorescence line (in our case we chose the 6,678 Å and the 6,402 Å line for He and Ne, respectively) are synchronously detected as the various Zeeman-split levels are saturated. For the example given here, we used a cell containing 100 μm of ^{3}He. A typical experimental run is shown in Figure 10. For this run, the static field was slowly swept with the simultaneous application of rf to the ground state and the metastable Larmor coils; again, a square wave was applied to the former coil for field calibration purposes. In the scan we were able to identify the $1^2S_{1/2}$ resonance of $^3He^+$. The lower fill pressure results in a smaller charge exchange collision rate, giving a longer $^3He^+$ lifetime, and thereby increasing the S/N ratio. The observation of the $^3He^+$ resonance indicates the sensitivity of the OPA technique.

The ground-state nuclear polarization at this lower pressure (100 μm) was measured (using the pump light intensity technique) to be 3.6%, as compared with a value of 9.5% for a 900 μm ^{3}He fill pressure. The value of the optical polarization asymmetry (at 6,678 Å) was measured to be $\sim 10^{-3}$, indicating a ~10% "efficiency" for the collisional transfer of the ground-state polarization to the higher lying states of helium. This is considered to be a reasonable value.

Finally, using the OPA technique, we have observed evidence of the "storage" of polarized ground state ^{3}He atoms in the ballast/reservoir region of the absorption cell. This was inferred from the long decay time (~40 to 60 sec) of the OPA signal when the 1.08 μm ^{4}He pump light was prevented from reaching the absorption cell. A typical result is shown in Figure 11. To establish a reference, rf at the Larmor frequency was first applied to an optically pumped ^{3}He cell, thus destroying the nuclear orientation. After the rf was removed,

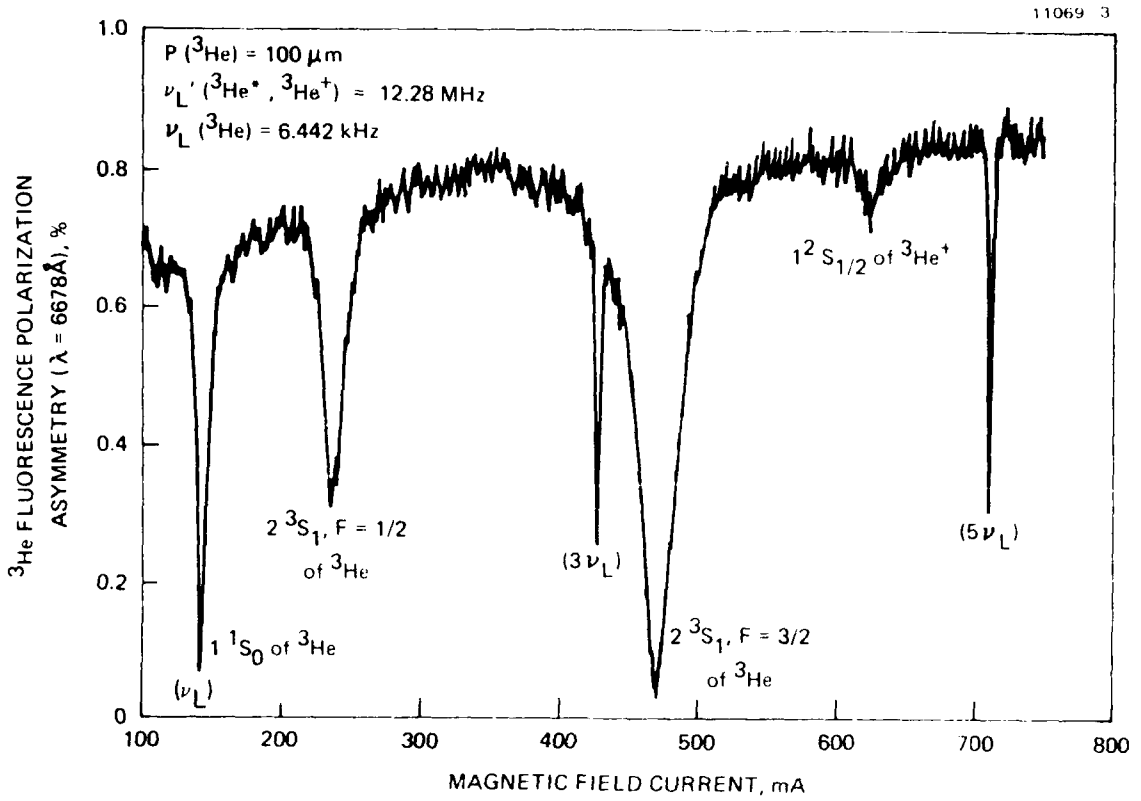

Figure 10. Observation of ^{3}He (ground state, metastable, and ground state ionic) resonances by scanning the applied magnetic field using the OPA technique.

the OPA signal built up (in ~60 sec) as the ^{3}He atoms again became optically pumped. At this point, the ^{3}He pump light was blocked and the long OPA decay was clearly indicated. (The OPA signal built up once again as the pump light was unblocked). We interpret this long decay time as follows: During the optical pumping cycle, polarized ^{3}He (1^1S_0) atoms diffuse through the capillary tube and reside (intact) within the ballast/reservoir region of the cell. After the pump light is blocked, some of these polarized atoms diffuse back into the discharge region and transfer part (~10%) of their polarization to the higher-lying ^{3}He states by collison.

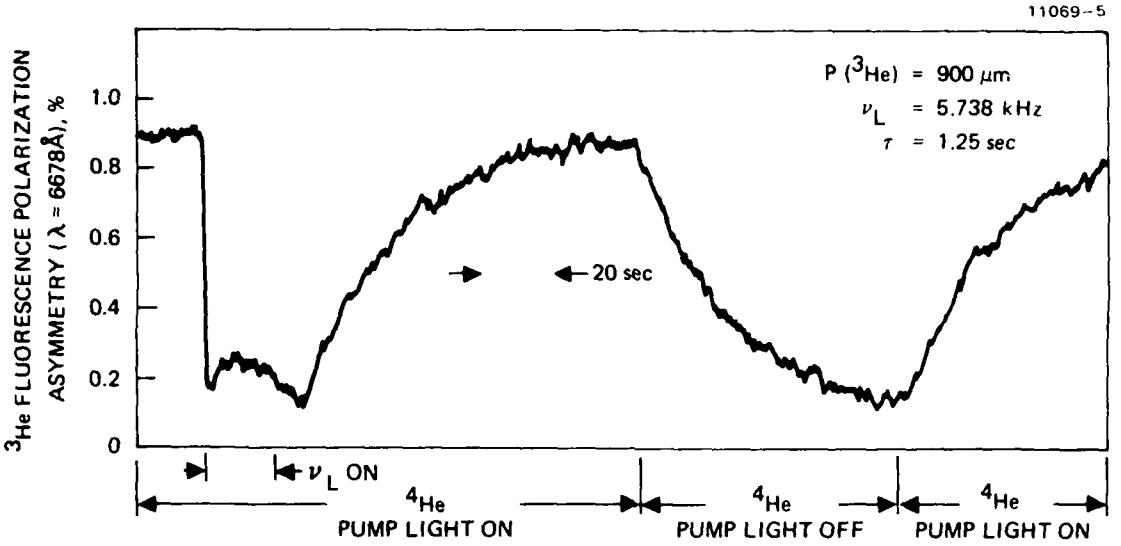

Figure 11. Decay of the OPA signal when the pump lamp radiation is prevented from incidence upon the absorption cell. The long decay time provided evidence of "storage" of polarized ground state ^{3}He atoms in the ballast region of the absorption cell.

We have also noted that absorption cells without ballast regions yielded short OPA decay times (~1 to 2 sec) as expected. (These measurements were possible through the use of the OPA technique; the pump light transmission scheme obviously could not be used in this case.) This is an important result in that it experimentally verifies the polarization storage mechanism, which is necessary for realization of the dumbbell-geometry NMR gyro sensor.

2. Optical Pumping of Binary Noble Gas Mixtures

In this section, we review experimental results that may provide a solution to the realization of an all-noble-gas, dual-isotope, low-cost, compact NMRG sensor. Since performance of the

sensor is directly proportional to the S/N ratios of the resonant transitions employed, significant polarization in both isotopic species that comprise the sensor is a critical requirement. Moreover, for a low-cost, compact geometry, a single optical pumping source that can simultaneously polarize both working species is desirable. Finally, narrow linewidths are essential to yield the required system performance. The successful experimental results to be discussed in this section appear to present a solution to these constraints. A more detailed discussion of these results is given in Appendix A, which is a preprint of a journal manuscript on this topic.

We have observed collision-induced polarization transfer from optically pumped helium to excited states of neon (as discussed in Section 2.B and presented in Figure 5). The $2\,^3S_1$ helium metastable state, being in close energy coincidence with the $2p^5 4s$ manifold of neon when optically pumped (at 1.08 μm), can transfer polarization to the neon atom. By cascade optical transitions, part of this polarization is preserved, being transferred to lower lying neon levels. When the polarization of an absorption cell neon spectral line is monitored, the polarization of the upper level (of the fluorescence line) becomes apparent. The presence of optical polarization here indicates the transfer of angular momentum from the directly pumped species (He) to the "buffer" gas (Ne).

In this study, (direct) optical pumping of helium was accomplished using a ^{4}He pump lamp. The emission at 1.08 μm was made circularly polarized, irradiating an absorption cell containing a mixture of helium (at 300 μm) and neon (at 5 μm). For these measurements, four cells were used containing various isotopes of both species: ^{4}He-^{20}Ne, ^{4}He-^{21}Ne, ^{3}He-^{20}Ne, and ^{3}He-^{21}Ne. The mechanism of polarization transfer from helium to neon was experimentally established by synchronously detecting the OPA signal of the absorption cell fluorescence line of neon at 6,402 Å along the quantization axis.

In all four cases the OPA signal decreases (i.e., the neon fluorscence becomes isotropic) whenever the "source" of polarization (helium) is depolarized. The magnitude of the signal (~1%) was observed to be independent of the neon or helium isotopic composition used. Moreover, the measured ^{3}He ground state polarization (~6.5%) was not significantly degraded using 5 μm of neon in the absorption cell. This was confirmed by using a test cell containing only ^{3}He (at 300 μm); the measured polarization was also ~6.5% (within our experimental error of ±0.5%). Finally, He-Ne absorption cells containing 200 μm of both He and Ne were tested. It was found that the collision-induced excited state neon polarization was down by a factor of three relative to the previous cells (containing 300 μm and 5 μm of He and Ne, respectively). We attribute this reduced value to collision-induced polarization relaxation effects of both He and Ne by neon. Thus, the optimal fill pressure for the simultaneous polarization of such binary gas mixtures will most likely require reduced neon fill pressures (<200 μm) and increased He densities (>200 μm), subject to relaxation effects and absorption cell discharge conditions (i.e., weak discharge, and sufficient He metastable densities). These observations of collisional angular momentum transfer are significant for several reasons:

- The all-gaseous ^{3}He and ^{21}Ne system can be polarized using only a <u>single</u> optical pumping source (at 1.08 μm). Combined with the elimination of a metallic vapor (Rb, Hg, etc.), which can lead to detrimental effects on the gyro performance, this technique is important for practical device applications.

- The near-energy coincidence of metastable (2^3S_1) helium with the excited state ($2p^54s$) manifold of neon results in a very efficient collision-induced transfer of polarization from optically pumped He to Ne.

- This transfer mechanism is not materially degraded when using odd isotopes for one or both of the interacting species.
- The polarization of ground-state ^{3}He is not significantly degraded by the presence of neon in the system.

These results lead us to expect a reasonably large nuclear polarization in the ground state of ^{21}Ne. Thus, we expect that a pair of polarized ground-state species (^{3}He and ^{21}Ne) can be simultaneously created, using a compact, lightweight geometry. This can result in a fast warm-up, inexpensive tactical gyro sensor.

3. Direct rf NMR Detection

One of the key thrusts of this program was to construct an apparatus capable of detecting ground state Zeeman resonances using rf NMR techniques. As mentioned earlier, we fabricated an electronics package capable of detecting a polarization of 10^{-3} in one Torr of helium at a S/N ratio of 2 (the "noise" in this case was measured by grounding all inputs to the receiver front end).

Prior to employing this approach, the dual-chamber absorption cells were tested by detecting the ^{3}He ground state resonance using the optical techniques discussed above. In addition, using the OPA technique, it was verified that polarized ground state ^{3}He atoms were stored in the observation region, with observed storage times consistent with calculations (~ 0.5 to 5 seconds, dependent on geometrical factors).

The presence of the resonances using optical techniques also confirmed that the absorption cells were properly fabricated and that the experimental apparatus was functional and calibrated. Parameters such as the dc magnetic field, the second order correction coils, absorption cell discharge conditions, pump lamp conditions, and other laboratory apparatus were evaluated in this manner.

Unfortunately, we were unable to detect the Zeeman resonances using rf NMR techniques. Systematic efforts such as varying the Larmor resonance frequency (by changing the receiver coil LC values, magnetic field settings, etc.), degaussing the permalloy magnetic shields, modifying the absorption cell discharge conditions, and reversing the sense of the magnetic field (in the case of FID studies) revealed no detectable signal. In the course of this investigation, all three rf detection schemes (mentioned in the previous section) were employed. In the case of the FID technique, both the stimulating pulse amplitude and pulse duration were varied. We note that the stimulating pulse frequency was derived from a frequency synthesizer (having a stability of better than 10^{-7}). Hence, stability of the stimulating signal was not a source of error. It was noted that the FET switching network weakly stimulated the receiver coil upon transitions between the stimulating and receiving mode. To circumvent this problem, reed relays were employed in place of the FET switches. Although this reduced the transient effects, the NMR signals were still not detectable. Finally, a second coil was wound co-axial relative to the receiver coil; this coil served as a separate stimulating coil. In this case, no switching problems were encountered; however, no resonance signals were observed.

We attribute the lack of a detectable signal to two systematic sources: environmental noise/transients, and magnetic field factors. We noted a periodic stimulating signal from the receiver even during the steady-state operation mode of our detection electronics (i.e., no injected pulses, etc.). These background signals were present even when we operated the receiver using a battery pack. Moreover, placing both the receiver front-end pre-amplifier and coil in a copper shield, and inserting this apparatus in a permalloy magnetic shield did not appreciably reduce the noise problem.

The ground state helium-3 NMR signals have been previously reported.[4,5,6] However, the observations were carried out using magnetic fields considerably higher than the maximum fields that our apparatus was designed to supply. The increased Larmor frequencies afforded by greater magnetic fields enables one to more efficiently shield the apparatus. Moreover, the background noise components at the higher operating frequencies is lower. This, coupled with the increased predicted NMR induced EMF, as well as the greater receiver coil Q attainable at higher frequencies, should improve the signal-to-noise ratio by several orders of magnitude. We believe that this improved system performance enabled previous workers to observe the various resonances.

The second major area of improvement relates to the dc magnetic field apparatus: magnetic field homogeneity (both spatially and temporally) and absorption cell aspect ratio. Although the observation of the "storage" of polarized ^{3}He atoms implies a sufficient degree of field homogeneity, further increasing the uniformity of the field would result in decreasing magnetic-field-dependent relaxation rates (as well as reducing the atomic resonance linewidth). Hanson and Pipkin[15] have shown that the magnetic field homogeneity in a shielded solenoid is critically dependent on the presence (and shape) of the shield end-caps. This factor is more critical than the presence of the cylinderical portion of the shield. Although our shield consisted of both end-caps and a cylinderical section, the resultant field distribution was probably degraded due to the fact that our end-caps were curved as opposed to being flat. Finally, the relaxation rates can be further decreased by using absorption cells of smaller volume, thereby occupying a smaller fraction of the solenoid volume. However, care must be taken to ensure a weak, uniform discharge (which will surely be affected by modifying the cell geometry) in the absorption cell.

SECTION 3

CONCLUSION AND SUGGESTIONS FOR FUTURE INVESTIGATIONS

During this program, we have identified the binary isotopic pair of ^{3}He and ^{21}Ne as being the optimal atomic species to realize an all noble-gas NMRG sensor. To this end, an apparatus was constructed to search for optically pumped Zeeman resonances in these atoms. Using an optical detection scheme, we observed such resonances in the ground state, metastable state and ionic ground state of ^{3}He, and in the metastable state of ^{21}Ne. In addition, we observed evidence of the "storage" of polarized ground state ^{3}He in the observation region of a dual-chamber absorption cell. This is a necessary condition for the realization of a narrow linewidth NMRG sensor. We were also able to simultaneously polarize a binary mixture of ^{3}He and ^{21}Ne in a common absorption cell using a single optical pumping source (^{4}He at 1.08 μm). This could lead to a compact device geometry. Moreover, the degree of polarization in this mixture was comparable to a naturally abundant He-Ne system (despite the more complex hyperfine spectra of the odd isotopes). Further, the polarization of the ^{3}He ground state atoms was not materially affected by the presence of the ^{21}Ne atom (for our operating fill pressures). This indicates the high degree of polarization attainable in such systems. An apparatus was also constructed to detect polarization using conventional rf NMR techniques. Although we were unable to observe ^{3}He resonances using this technique, we identified potential noise sources and systematic effects that should enable us to detect ground state NMR signals. Indeed, since previous workers have observed resonances in ^{3}He using similar techniques (at higher operating frequencies, however), we have confidence that a dual isotope NMRG sensor can be realized. Finally, performance estimates were determined for the frequency and linewidth precisions necessary to achieve the desired NMRG angular rate resolution. We showed that, for the

polarizations attainable, the performance requirements can indeed be satisfied.

In terms of future investigations, an attempt to scale our apparatus to higher operating frequencies would be a valuable exercise, both to observe the various resonance and to circumvent systematic experimental deficiencies. Furthermore, alternate optical pumping sources need attention. Color center lasers[16] and/or semiconductor lasers[17] offer the potential for increased efficiency, reduced weight, cost, and size. Finally, using techniques such as optogalvanic[18,19,20] detection should provide the stabilization[21] accuracy necessary to achieve efficient, cost-effective locking of the source to the optical pumping species. These approaches and techniques should enable the NMRG sensor to evolve into a viable, tactical system.

REFERENCES

1. J. Brossel, Quantum Electronics III, edited by P. Grivet and N. Bloembergen (Columbia University Press, 1964), pp. 201-212; R.C. Greenhow, Phys. Rev. A 136, 660 (1964); R.S. Timsit and J.M. Daniels, Can. J. Phys. 49, 545 (1971).

2. J. Brossel, Fundamental and Applied Laser Physics, edited by M.S. Field, A. Javan, and N. Kurnit (Wiley, 1973), p. 769-790.

3. C.H. Volk, T.M. Kwon, J.G. Mark, Y.B. Kim, and J.C. Woo, Phys. Rev. Lett. 44, 136 (1980).

4. H.G. Robinson and Than Myint, Appl. Phys. Lett. 5, 116 (1964).

5. G. Escher and P. Turowski, Z. Angew. Phys. 21, 50 (1966); P. Bley and P. Turowski, Z. Angew. Phys. 24, 57 (1967).

6. R.A. Zhitnikov, I.A. Kravtov, and M.P. Fradkin, Sov. Phys. Tech. Phys. 20, 955 (1976); ibid. 22, 377, 381, and 384 (1977).

7. B.C. Grover, Phys. Rev. Lett. 40, 391 (1978).

8. E.J. Robinson, J. Levine, and B. Bederson, Phys. Rev. 146, 95 (1966).

9. F. Sage, J.P. Lemoigne, and D. Lecler, Opt. Comm. 30, 332 (1979); A. Noel, M. Leduc, and F. Laloe, CRAC 274, 77 (1972).

10. L.D. Schearer, Phys. Lett. 27A, 544 (1968); Phys. Rev. Lett. 180, 83 (1969).

11. D.M. Pepper, and H.T.M. Wang, "Nuclear Magnetic Resonance Gyroscope," Techical Report, December 1982, AFOSR Contract No. F49620-80-C-0046.

12. J. Duppont-Roc, M. Leduc, and F. Laloe, Phys. Rev. Lett. 27, 467 (1971).

13. See, for example, A. Abragam, The Principles of Nuclear Magnetism (Clarendon, Oxford, 1961); Farren and Becker, Pulse and Transform NMR (Academic Press, New York, 1971), Ch. 2.

14. L.D. Schearer, Phys. Rev. 188, 505 (1969).

15. R.J. Hanson and F.M. Pipkin, Rev. Sci. Inst. 36, 179 (1965). See also L.C. Balling in Advances in Quantum Electronics, Vol. 3, D.W. Goodwin, ed. (Academic Press, New York, 1975), pp. 1-167.

16. K.W. Giberson, C. Cheng, M. Onillion, F.B. Dunning, and G.K. Walters, Rev. Sci. Instrum. 53, 1789 (1982).

17. D.D. McGregor, AFOSR Contract No. F49620-78-C-0056.

18. R.B. Green, R.A. Keller, G.G. Lutha, R.K. Schenci, and J.C. Travis, Appl. Phys. Lett. 29, 727 (1976); W.B. Bridges, J. Opt. Soc. Am. 68, 352 (1978).

19. D.M. Pepper, IEEE J. Quantum Electron. QE-14, 971 (1978).

20. C. Stancivlescu, R.C. Bobulescu, A. Surmeian, D. Popesov, I. Popescu, and C.B. Collins, Appl. Phys. Lett. 37, 888 (1980).

21. S. Yamaguchi and M. Suzuki, Appl. Phys. Lett. 41, 597 (1982).

APPENDIX A

POLARIZATION TRANSFER BETWEEN ORIENTED METASTABLE HELIUM ATOMS AND NEON ATOMS: A COMPARISON OF EVEN AND ODD ISOTOPES.

David M. Pepper and Harry T.M. Wang

Hughes Research Laboratories
3011 Malibu Canyon Road
Malibu, California 90265

ABSTRACT

Collision-induced polarization transfer from optically pumped helium to excited states of neon is studied using various combinations of even and odd isotopes. It is found that, within our experimental accuracy of 10%, the resultant polarization is independent of the isotopic composition of the binary mixture. Possible applications using this mechanism are discussed.

The field of optical pumping has been investigated extensively over the past several decades.[1] One area that has received much attention involves the effects of angular-momentum-conserving collisions on the transfer of polarization (i.e., Zeeman population differences) among various species in an optically pumped gaseous mixture. Indeed, when a polarized atom collides with a similar (or different) unpolarized species, spin exchange accompanying the energy transfer can occur. Collision-induced polarization transfer has been observed between like neutral atoms (e.g., noble gases) in weak discharges,[2,3] via charge exchange collisions,[4] Penning collisions,[5] and molecular fragmentation,[6] to mention a few mechanisms. Schearer[7] reported the observation of collisionally-induced spin exchange between optically pumped metastable helium atoms and various excited states of neon atoms in a naturally abundant mixture (primarily ^{4}He-^{20}Ne, possessing nuclear spin I=0 for both species).

In this letter, we report a polarization transfer scheme similar to that of Schearer[7] in a He-Ne mixture, but as a function of the isotopic composition of the species. We find that, within experimental accuracy, the resultant polarization transfer to selected excited states of neon is essentially independent of the isotopic composition. One may conjecture that, due to the more complex (hyperfine) energy level structure of noble gas atoms possessing nuclear spin, the efficiency of the polarization transfer process would decrease (due to inter-atomic collisions, etc.) relative to isotopes without nuclear spin. Since we do not see this trend, the atomic ensemble is most likely within the collision-dominated regime,[8] presumably due to the discharge conditions and the partial pressures used in our absorption cells.

Moreover, we measured the excited state neon polarization to be ~1%, which is a factor of five greater than that obtained using direct optical pumping of metastable neon.[9] One therefore expects that, via metastability exchange collisions [1,10] between

between polarized metastable neon and ground state neon atoms, a large density of oriented ground state neon atoms should result; this could be far in excess of the ground state ^{21}Ne polarization measured[3] ($\sim 10^{-5}$), which involved direct neon optical pumping techniques similar to that used in helium.[1]

It should therefore be possible to efficiently and simultaneously polarize the ground states of both ^{3}He (I=1/2)and ^{21}Ne (I=3/2) in a binary mixture using a single optical pumping source (e.g., ^{4}He at λ = 1.08 μm). The realization of this effect could have a profound impact in the fields of fundamental study and applied physics.

Schearer[7] previously found that optically pumped metastable ^{4}He atoms (2^3S_1) can transfer polarization to excited ^{20}Ne atoms ($^1S_0$) in collisions of the second kind occurring in a cell containing He and Ne (see Figure A-1). As a result of such collisions, energy is transferred to the $2p^5 4s$ manifold of neon. Due to cascade radiative transitions, part of this polarization is preserved and is transferred to various lower lying excited states of neon. In our experiment, we detected the polarization by monitoring the circular optical polarization asymmetry (OPA) along the quantization axis of an isolated neon fluorescence line at 6,402 Å (the $2p_9 \rightarrow 1s_5$ transition, in Paschen notation).

Our experimental apparatus is shown in Figure A-2. Metastable (2^3S_1) He atoms are created in a He-Ne absorption cell when driven by a weak rf electrodeless discharge (~5 m W at ~150 MHz). The 2^3S_1 state of He is optically pumped by irradiating this cell with circularly polarized resonant light at 1.08 μm. The source of the pumping light is a cell containing ~2 Torr of ^{4}He, driven by a strong, rf electrodeless discharge (~100 W, at ~30 MHz). The pump light is rendered circularly polarized upon propagation through a Polaroid HR-type linear polarizer, followed by a quarter wave plate (a stack of 140 nm Polaroid retarder plates). The light is filtered (using a Kodak #87C filter) to allow passage of the 1.08 μm component, while blocking visible

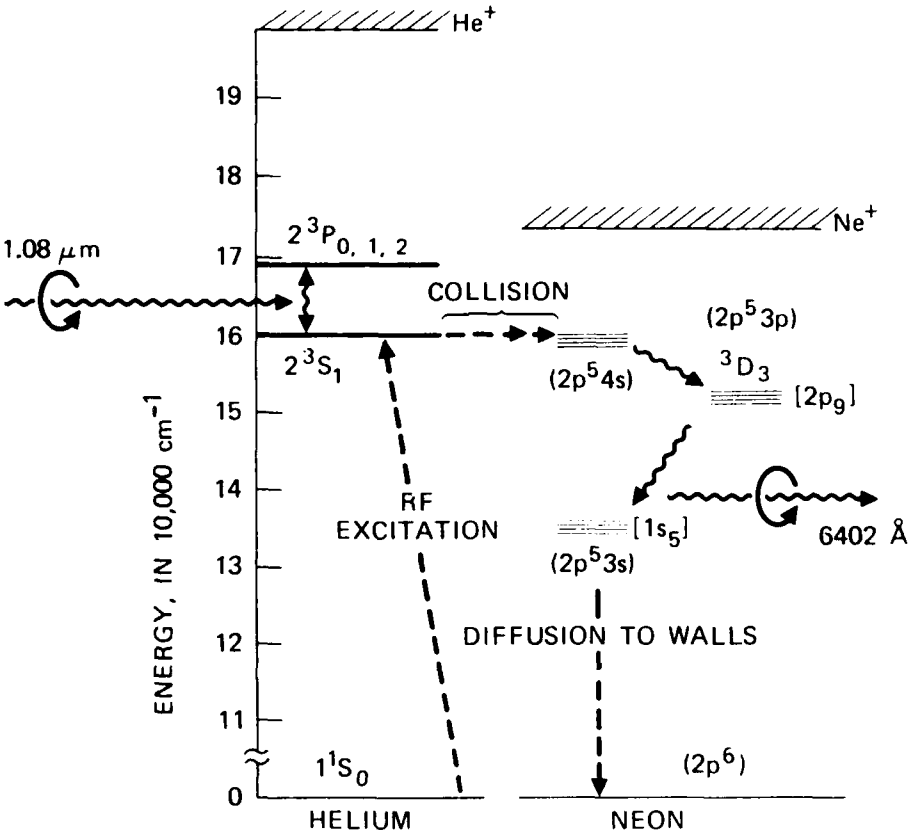

Figure A-1. Relevant energy level diagram in a He-Ne system. Circularly polarized 1.08 μm pump light spin orients 2^3S_1 helium metastable atoms. Part of the resultant polarization is collisionally transferred to neon, resulting in a circular optical polarization asymmetry (OPA) of various neon fluorescence lines (e.g., 6402 Å). [ ]: Paschen notation; ( ): electronic shell configuration.

12918 1

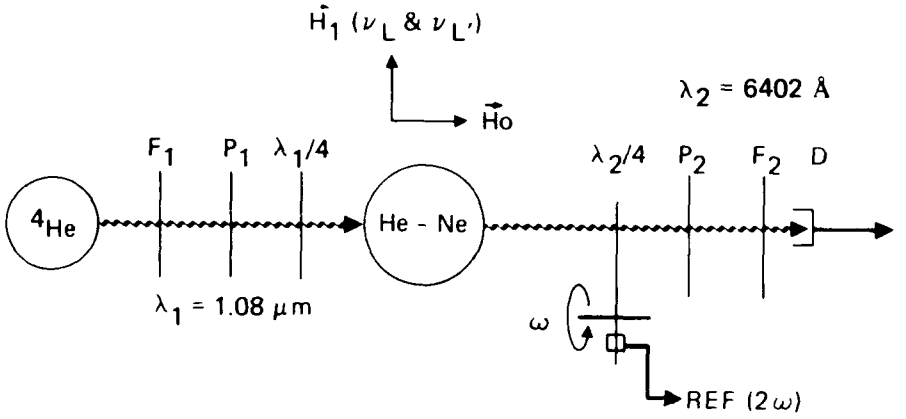

Figure A-2. Basic experimental apparatus. Pump light (at λ = 1.08 μm) from an electrodeless rf discharge (in ^{4}He) is rendered circularly polarized, and irradiates a cell containing a He-Ne mixture (driven by a weak electrodeless discharge), placed in a dc magnetic field, H_o. Magnetic resonances are observed by synchronously detecting circular polarization changes (at 2ω) of the neon fluorescence (λ = 6,402 Å) as H_o is slowly scanned, in the presence of Larmor frequencies, ν_L and $\nu_{L'}$. F_i: line filters; P_i: linear polarizer; $\lambda_i/4$: quarter-wave plates (i = 1,2 corresponds to 1.08 μm and 6,402 Å, respectively); D: detector.

lines. Lenses and a quartz lightpipe are used to couple the 1.08 μm pumping light into the absorption cell. The absorption cell is situated in a permalloy shielded, longitudinal dc magnetic field solenoid (corrected to second order), which is variable from ~1 to 10 gauss. The absorption cell is also surrounded by a pair of coils to couple rf at the various Larmor frequencies (in the kHz and MHz ranges, for the Zeeman-split nuclear and electronic levels, respectively). The 6,402 Å neon

fluorescence light emitted from the cell is sychronously detected using narrow bandpass filters and an EMI 9558QB photomultiplier tube. The circular optical polarization asymmetry of this radiation is measured by first passing the 6,402 Å light through a rotating quarter-wave plate (at ω), followed by a linear polarizer. This results in an amplitude modulated signal (at 2ω), with a depth of modulation depending on the amount of OPA.

In our study, four absorption cells were used, containing various isotopic mixtures of helium (at 300 μm pressure) and neon (at 5 μm pressure): ^{4}He-^{20}Ne, ^{4}He-^{21}Ne, ^{3}He-^{20}Ne and ^{3}He-^{21}Ne. Figures A-3 through A-6 show experimental results for the respective absorption cells. In these figures, we plot the synchronously detected neon 6,402 Å OPA amplitude as a function of the dc magnetic field strength. This is recorded in the presence of saturating rf applied to the absorption cell Larmor coils at frequencies of 11.45 MHz (sine wave) and 492 Hz (square wave). The former signal couples to the (electronic) Zeeman-split levels of the $2^{3}S_{1}$ metastable state of $^{3,4}He$, while the latter signal couples to the (nuclear) Zeeman-split ground state of ^{3}He. The odd harmonics of the square wave couple to the Zeeman-split levels at correspondingly higher magnetic field strengths; these signals are used for reference purposes of ground state ($1^{1}S_{0}$) ^{3}He.

The ground state ^{3}He atoms become polarized by virtue of angular momentum-conserving metastability exchange collisions[17] (between $1^{1}S_{0}$ atoms and polarized $2^{3}S_{1}$ atoms). Hence, the metastable He atoms (and additionally, the ground state atoms in the case of ^{3}He) act as a "reservoir" of stored angular momentum which can be transferred to excited state neon atoms via collisions of the second kind.

Referring to the experimental results, note that the OPA signal decreases (i.e., the neon flourescence becomes isotropic) whenever the "source" of polarization (i.e., the oriented helium

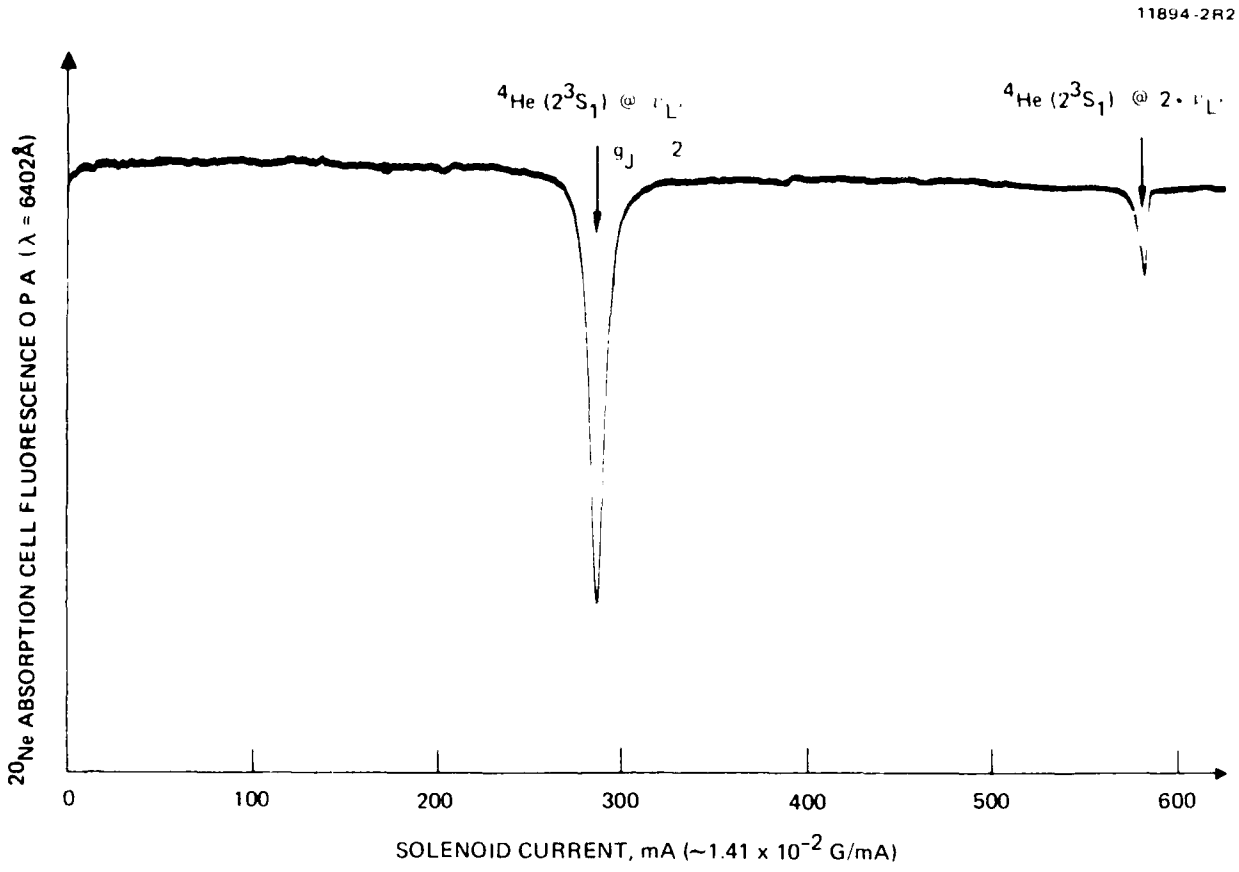

Figure A-3. Polarization transfer from optically pumped ^{4}He to ^{20}Ne. Helium Zeeman resonances in a cell containing a mixture of ^{4}He and ^{20}Ne are detected by observing the polarization of the 6,402 Å emission line of ^{20}Ne. In all cases, the magnetic field solenoid current sweep rate was 100 mA/100 sec; lock-in time constant was 4 sec; $\lambda/4$ rotation rate was 18 Hz. All lamps were pyrex. The calculated Landau g-factors are noted in all the figures.

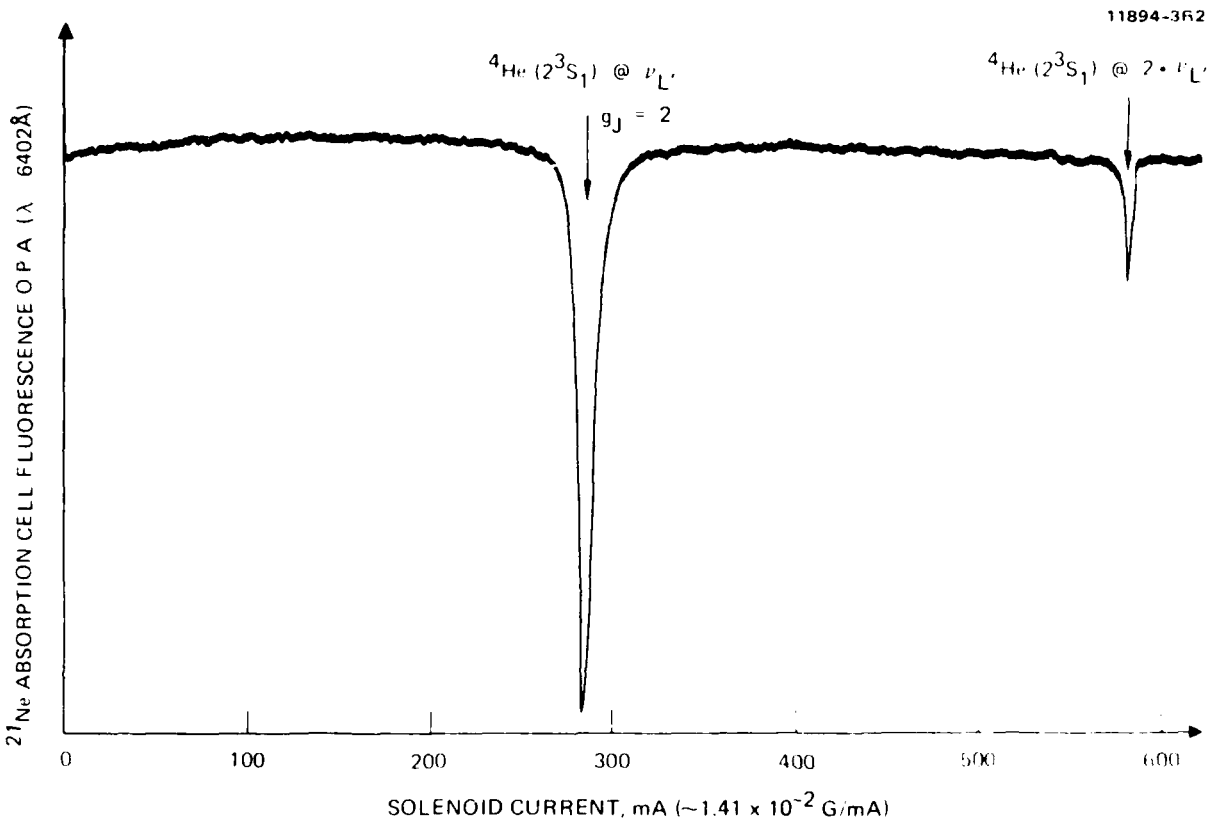

Figure A-4. Polarization transfer from optically pumped ^{4}He to ^{21}Ne. Helium Zeeman resonances in a cell containing a mixture of ^{4}He and ^{21}Ne are detected by observing the polarization of the 6,402 Å emission line of ^{21}Ne.

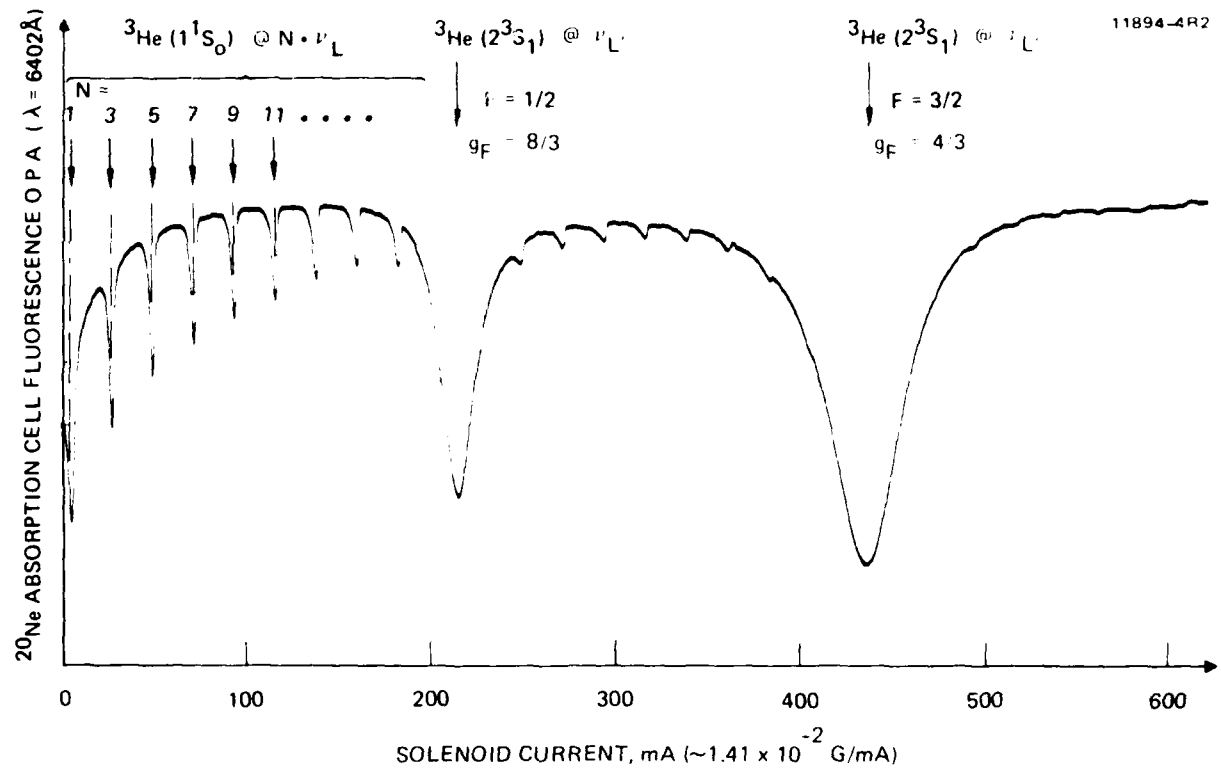

Figure A-5. Polarization transfer from optically pumped ^{3}He to ^{20}Ne. Helium Zeeman resonances in a cell containing a mixture of ^{3}He and ^{20}Ne are detected by observing the polarization of the 6,402 Å emission line of ^{20}Ne.

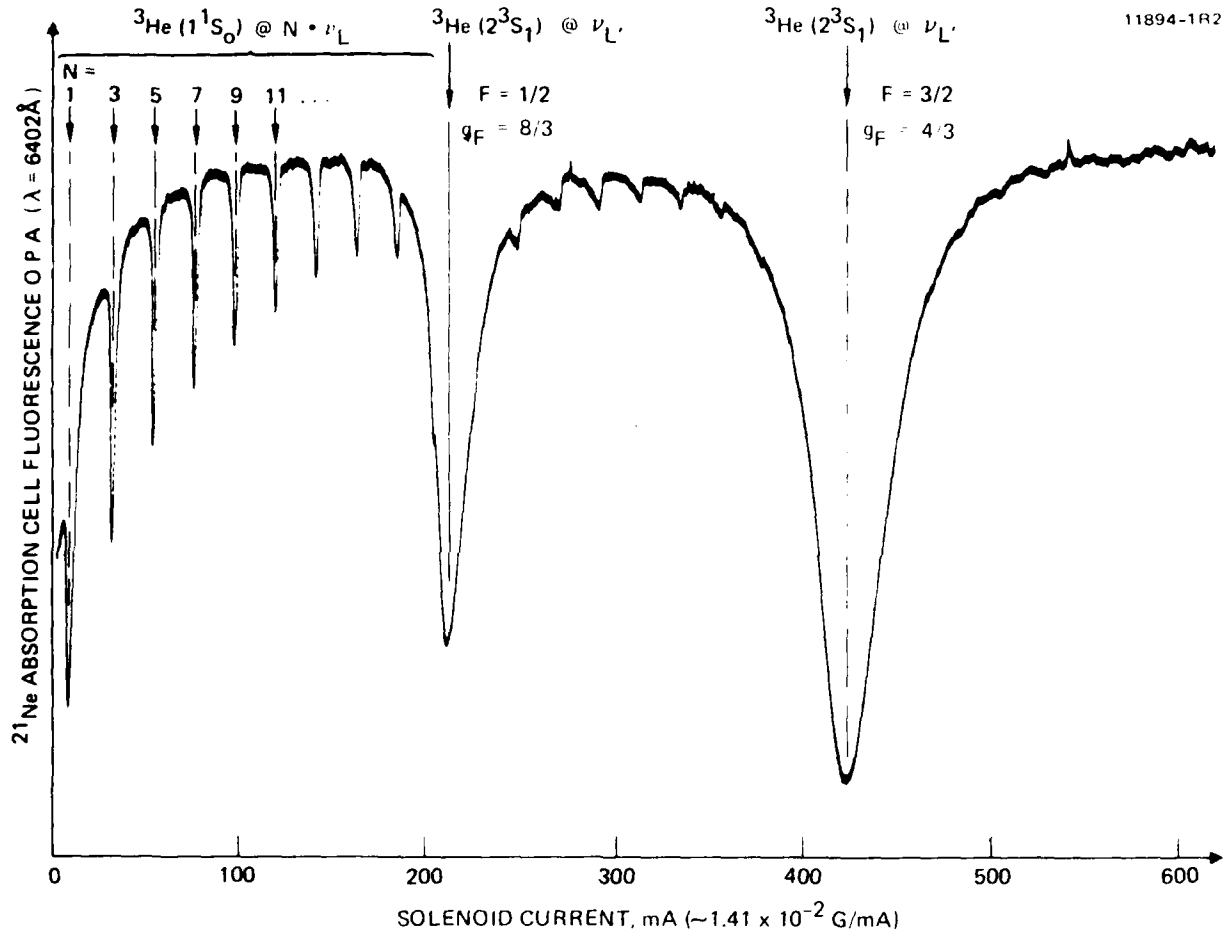

Figure A-6. Polarization transfer from optically pumped ^{3}He to ^{21}Ne. Helium Zeeman resonances in a cell containing a mixture of ^{3}He and ^{21}Ne are detected by observing the polarization of the 6,402 Å emission line of ^{21}Ne.

atoms) is depolarized. The OPA signals also vanish when the ^{4}He pump lamp is extinguished. All the resonances are power roadened due to the application of saturating rf at the Larmor frequencies.

In Figures A-3 and A-4, cells containing mixtures of ^{4}He-^{20}Ne and ^{4}He-^{21}Ne were evaluated. In both cases, where ^{4}He is the optically pumped species, the Zeeman resonance of the ^{4}He metastable state (2^3S_1) is clearly seen. We note that the signal at $2 \cdot \nu_L'$ is due to an intentionally produced second harmonic distortion component of the highly driven rf amplifier at 11.45 MHz, and is used for reference purposes. The magnitude of the signals (~1%), coupled with the excellent signal-to-noise (S/N) ratio, provide evidence that the upper level of the 6,402 Å transition (the neon $^3D_3$ state) is strongly polarized, as is the 2^3S_1 state of ^{4}He.

The similarity of Figures A-3 and A-4, in terms of S/N ratio and magnitude, indicates that the resultant $^3D_3$ Ne polarization is comparable for both ^{20}Ne and ^{21}Ne (despite the more complex hyperfine spectrum of ^{21}Ne). This same result is evident by comparing Figures A-5 and A-6, where cells containing mixtures of ^{3}He-^{20}Ne and ^{3}He-^{21}Ne were used. In this set of experimental runs, ^{3}He is the optically pumped species. The resultant ^{3}He spectrum, showing the 1^1S_0 ^{3}He ground state and associated odd harmonics of the (square wave) Larmor signal, along with the two 2^3S_1 metastable resonances, again indicates that the polarization transfer mechanism is comparable using either odd or even neon isotopes.

In this study, the OPA detection technique is insensitive to the ground and the metastable neon Zeeman resonances. The reason for this is the tight coupling of the OPA signal to the source of atomic angular momentum (He). Thus, ground and metastable helium resonances which perturb the reservoir of atomic angular momenta in the optical pumping cell are easily observed, since

polarization transfer is from helium to the $2p^5 4s$ levels of neon. The perturbation on the polarization of these neon levels and other shortlived excited states caused by ground and metastable neon resonances will be quite small, by at least the ratio of the lifetimes. However, it should be possible to observe the polarization of the neon metastable and ground states by direct optical and rf nuclear magnetic resonance detection techniques, respectively.

The magnitude of the excited state neon optical polarization (~1%) is approximately a factor of 5 greater than that obtained in direct optical pumping of neon metastables (i.e., by using circularly polarized 6,402 Å pump light).[9] This fact reveals the high efficiency of both the collisionally-induced polarization transfer mechanism from He to Ne, as well as the direct optical pumping efficiency of He.

Regarding the latter point, we measured the polarization of He directly using the pump light transmission method[4] (i.e., monitoring changes in the steady-state metastable absorption of pump light with and without the application of resonant Larmor fields). The measured values of ~6.5 (±0.5)% using He-Ne absorption cells compare favorably (within experimental uncertainty) with that of an absorption cell containing pure He. Hence, at the fill pressure we used, the He polarization is weakly perturbed by the presence of neon in the absorption cell.

In another set of runs, a cell containing 200 μm of both He and Ne was evaluated. In this case, the Ne polarization was reduced by a factor of three relative to that obtained using the above cells. This reduced value can be attributed to either of two effects: (1) collision-induced depolarization of helium (and/or neon) by neon; or (2) a decreased steady-state helium metastable population, due to differences in the He-Ne discharge conditions. Hence, one anticipates that cells containing neon in the range of 5 μm to 200 μm (with possibly increased He pressures) can be used to optimize the density of polarized atoms. Note however, that the density of He metastables (as well as excited state polarization densities) depends critically on

on both the partial pressures (of both species), as well as on the discharge conditions.

These observations are significant for several reasons. First, an all gaseous He-Ne system can be polarized using only a single optical pumping source (at 1.08 μm). We note that a color center laser has been recently used[11] to efficiently optically pump helium. Second, the near-energy coincidence of metastable (2^3S_1) helium with the excited state ($2p^5 4s$) manifold of neon results in a very efficient collision-induced transfer of polarization from optically pumped He to Ne. This transfer mechanism is not materially degraded using odd isotopes for one or both of the interacting species (despite the more complex hyperfine spectrum of the odd isotopes). Additionally, the polarization of ground-state ^{3}He is not significantly degraded by the presence of neon in the system (at our operating pressures). Finally, due to the large excited-state neon polarization, one expects significant polarization of neon metastables. This can lead to a large number density of polarized ground-state ^{21}Ne atoms by a metastability exchange collision process between metastable and ground state neon atoms (in an analogous manner as that occurring in helium). The degree of polarization is expected to be far greater than that observed using direct optical pumping techniques.

In conclusion, we have observed significant collision-induced transfer of polarization between oriented helium and excited states of neon in a binary mixture of He and Ne. Since the observed result is independent of the isotopic composition of the mixture, one expects significant ground state polarization of ^{21}Ne. This result has implications in terms of fundamental studies (i.e., measuring Landau g-factors, atomic spectroscopy, collision phenomena, polarized particle beams, etc.) and practical applications (rf masers, magnetometers, gyroscopes, etc.).

The authors wish to acknowledge the technical assistance of T. Calderone, C. Fetters, J. Lewis, and L. McNulty. This effort was supported in part by AFOSR contracts F49620-80-C-0046 and F49620-82-C-0095 and by Hughes Aircraft Company.

REFERENCES

1. For reviews, see, for example, J. Brossel, Fundamentals and Applied Laser Physics, M.S. Field, A. Javas, and N. Kurmit, eds. (Wiley, 1973), pp. 769-790; W. Happer, Rev. Mod. Phys. 44, 169 (1972); L.C. Balling in Advances in Quantum Electronics Vol. 3, D.W. Goodwin, ed (Academic Press, New York, 1975), pp. 1-167; B. Decomps, M. Dumont, and M. Ducloy, "Linear and Nonlinear Phenomena in Laser Optical Pumping," in Topics in Applied Physics Vol. 2, Laser Spectroscopy of Atoms and Molecules, ch. 5, pp. 283-347 (Springer-Verlag, Berlin, 1976). Recent theoretical work work is given by S.V. Bozhokin and B.G. Matisov, Opt. Spect. 52, 77 (1982).

2. F.D. Colegrove, L.D. Schearer, and G.K. Walters, Phys. Rev. 132, 2561 (1963).

3. F. Sage, J.P. Lemoigne, and D. Lecler, Opt. Comm. 30, 332 (1979); A. Noel, M. Leduc, and F. Laloe, CRAC 274, 77 (1972).

4. M. Leduc and F. Laloe, Opt. Comm. 3, 56 (1971).

5. See, for example, L.D. Schearer and L.A. Reiseberg, Phys. Lett. 35A, 267 (1971); L.D. Schearer and W.F. Parks, in Prog. in Atomic Spect. 13, W. Hanle and H. Kleinpopper, eds. (Planum Publishing Corp, 1979), pp. 769-775; L.D. Schearer and W.C. Holton, Phys. Rev. Lett. 24, 1214 (1970); L.D. Schearer, Phys. Rev. Lett. 22, 629 (1969).

6. S.P. Dumitrieo, V.A. Kartoshkin, G.V. Klementev, V.D. Melnikov, and A.J. Okunevich, Opt. Spect. 51, 123 (1981); O.S. Vasyutinskii, Opt. Spect. 51, 124 (1981).

7. L.D. Schearer, Phys. Lett. 27A, 544 (1968).

8. For discussions of optical pumping and collisional processes, see, for example, A. Omont, Prog. Quant. Electronics 5, 69(1977); and E.L. Lewis, Physics Reports 58, 1 (1980).

9. L.D. Schearer, Phys. Rev. 180, 83 (1969).

10. J. Dupont-Roc, M. Leduc, and F. Laloe, Phys. Rev. Lett. 27, 467 (1971).

11. K.W. Giberson, C. Cheng, M. Orillion, F.B. Dunning, and G.K. Walters, Rev. Sci. Instr. 53, 1789 (1982).


ATE
LME